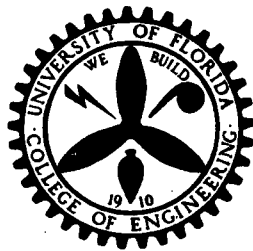


N 7 3 2 4 9 3 6

THERMODYNAMIC PROPERTIES OF UF_6
MEASURED WITH A BALLISTIC PISTON COMPRESSOR



CASE FILE
COPY

ENGINEERING AND INDUSTRIAL EXPERIMENT STATION

College of Engineering

University of Florida

Gainesville

SPECIAL REPORT

THERMODYNAMIC PROPERTIES OF UF_6
MEASURED WITH A BALLISTIC PISTON COMPRESSOR

By

David E. Sterritt
University of Florida

George T. Lalos
Naval Ordnance Laboratory
White Oak, Maryland

Richard T. Schneider
University of Florida

Work supported by

National Aeronautics and Space Administration
NGL 10-005-089

March 1973

Department of Nuclear Engineering Sciences
University of Florida

This work was supported by the National Aeronautics and Space Administration, NGL 10-005-089.

The authors wish to thank Dr. Karlheinz Thom (US AEC/NASA, Nuclear Systems Office) for his help and scientific contributions to this work during his three month stay at the University of Florida.

Thanks also go to Dr. Makoto Takeo, University of Oregon for supplying his simulation program and for helpful counseling in its use.

Credit for the design and testing of the pulse shaping network goes to Mr. Gordon Hammond of the US Naval Ordnance Laboratory, Silver Spring, Maryland.

The helpful advice of Dr. C. D. Kylstra, University of Florida, in the use of his optimization program is also acknowledged.

We also would like to thank Dr. Richard D. Dresdner, University of Florida for his advice and help regarding the physics and chemistry of UF_6 .

ABSTRACT

From experiments performed with a ballistic piston compressor, certain thermodynamic properties of uranium hexafluoride are investigated. Difficulties presented by the nonideal processes encountered in ballistic compressors are discussed and a computer code BCCC (Ballistic Compressor Computer Code) is developed to analyze the experimental data. The BCCC unfolds the thermodynamic properties of uranium hexafluoride from the helium-uranium hexafluoride mixture used as the test gas in the ballistic compressor. The thermodynamic properties deduced include the specific heat at constant volume, the ratio of specific heats for UF_6 , and the viscous coupling constant of helium-uranium hexafluoride mixtures.

TABLE OF CONTENTS

	Page
I. INTRODUCTION	1
II. EXPERIMENTAL APPARATUS	6
A. Ballistic Piston Compressor	6
B. Diagnostics	14
1. Measurement of Test Gas Pressure	14
2. Measurement of UF ₆ Pressure	14
3. Volume Measurement	17
4. Temperature Measurement	20
III. THEORETICAL REVIEW	24
A. Equation of State	24
B. Ratio of Specific Heats	25
C. Non-adiabaticity of the Compression Process	25
IV. ANALYTICAL TECHNIQUE	33
A. Piston Motion Simulation	33
B. Numerical Error Analysis of Piston Motion Simulation	43
V. DATA REDUCTION AND EXPERIMENTAL RESULTS	47
A. Method of Optimization	47
B. Organization of the Ballistic Compressor Computer Code	49
C. Calibration of the BCCC	49
D. Analysis of the Ratio of Specific Heats	51

Table of Contents (Continued)

	Page
E. Analysis of the Viscous Coupling of Uranium Hexafluoride and Helium	53
F. Results of Numerical Analysis of Experimental Data	58
VI. CONCLUSIONS	63
REFERENCES	64
APPENDIX A DETAILS ON THE COMPRESSION PROCESS	66
APPENDIX B PROGRAM (BCCC) LISTING	
APPENDIX C USER INSTRUCTIONS	
APPENDIX D TEST PROBLEM	

LIST OF FIGURES

Figure	Page
1. Ballistic Piston Compressor	7
2. Ballistic Piston Compressor (Reservoir End)	8
3. Ballistic Piston Compressor (High Pressure End)	11
4. Piston and Cup Seals	12
5. Gas Handling System	13
6. Data Acquisition System	15
7. Baseline, Calibration, and Pressure Traces	16
8. Trace of Magnetic Pickup and Amplifier Output	18
9. Diagram Illustrating Magnetic Pickup	19
10. Raw Data of Brightness Emissivity Temperature Measurement	22
11. Time Comparison of Minimum Volume and Maximum Pressure	23
12. Experimental and Calculated Temperatures Vs. Time	28
13. Flow Chart of BCCC Simulation	35
14. Moles of Test Gas During a Typical Experiment	52
15. Specific Heat Ratio Vs. Pressure	54
16. Specific Heat Ratio Vs. Temperature	55
17. Specific Heat Ratio Vs. Time	56
18. Viscosity of the Test Gas Mixture	59
19. Viscosity of the Test Gas Mixture as a Function of Pressure	60
20. P-V Diagram of the Compression Process	61
21. Ratio of Specific Heats of Uranium Hexafluoride	62

List of Figures (Continued)

Figure	Page
A-1. Heat Losses During Compression	67
A-2. Heat Losses as a Function of Pressure	68
A-3. Friction Work During Compression	69

LIST OF TABLES

Table	Page
1. Specific Heat at Constant Volume	3
2. Van der Waals' Constants of Helium and Uranium Hexafluoride	26
3. C_V Values for Helium and Uranium Hexafluoride	40
4. Results of Numerical Simulation without Gas Leakage or Heat Loss	50
5. Experimental Values of Specific Heat (C_V) and Viscous Coupling Constants (C_1)	57

I. INTRODUCTION

Gas-driven pistons in closed-end tubes can be used to study the properties of gases. Fast response detection systems for determining the volume, pressure, and temperature of the test gas have made this area of investigation into the properties of gases most rewarding. The U.S. Naval Ordnance Laboratory pioneered research into this field in the early sixties [1]. Successful numerical analysis of the phenomena observed in ballistic compressors was achieved by Takeo [2] in 1965 with the development of a computer program which calculates gas leakage past the piston and heat losses from the test gas to the walls of the compressor. Measurement of the time lag between the maximum pressure and the maximum light intensity at the University of Oregon [2] supplied new evidence for explaining the phenomena of gas leakage, past the piston during compression.

Using the initial work on numerical analysis done at the University of Oregon, the University of Florida has developed the BCCC which extracts the thermodynamic parameters of the test gas from experimental pressures, temperature, and volumes, each measured as a function of time.

The properties of uranium hexafluoride have been extensively investigated at temperatures below 500°K. The specific heat ratios, the specific heat at constant volume, the vapor pressures, entropy, and enthalpy have all been investigated and tabulated but only at low temperatures.

The specific heat ratios has been investigated by measuring the

velocity of sound and by measuring the ratio (C_p/C_v) at 50°C. This value is $1.063 \pm 0.5\%$.

Table 1 gives experimental measurements of the specific heat, C_v , of UF_6 vapor. Measurements of this parameter have, by and large, been done by spectroscopic techniques. The result of these investigations have resulted in values for the specific heat at constant pressure which are 10% lower than other experimental measurements.

Besides the obvious value of ballistic piston compressors in determining thermodynamic properties of gases at high pressures and temperatures, they can provide valuable information in other applied technology fields. The analysis of gases proposed for use in the gas core nuclear reactor is an excellent example of a low cost experiment to simulate conditions and analyze phenomena expected in large scale prototypes. In particular, the lifetimes of various species of gas molecules including that of uranium hexafluoride will be of extreme interest in the gas core reactor.

Another application of ballistic piston compressors is development of the nuclear piston engine. By simulating one stroke of the nuclear piston engine, a ballistic piston compressor can provide valuable information needed before a critical nuclear piston engine is constructed. Also, by using a nuclear reactor in conjunction with a ballistic piston compressor, the interaction of fission fragments and plasma may be studied. Since the plasmas obtainable with ballistic piston compressors are hot, dense, and long lived, they could provide a valuable research tool into those areas where plasma lifetime has previously been a major restriction.

Since the conditions of the test gas in a ballistic compressor

Table 1

Heat Capacity of the Vapor

Temperature °K	C_V/R							
	Source	11	12	13	14	15	16	17
100		8.53	8.44					
150		10.80	10.74					
200		12.46	12.40					
250			13.66	13.74				13.95
273		14.17	14.13	14.25				
273.2						13.70		
298		14.61	14.57	14.70				
298.2					15.86			
323		14.98	14.95	15.07				14.81
323.2						14.15	13.60	
348		15.30	15.27	15.38	16.37			
348.2						14.50		
378		15.58						15.51
398			15.79	15.89				
398.2					16.87			
400		15.84	15.81					
500		16.42	16.50	16.68				
650				17.54				
750		17.30						
1000		17.60						

change by several orders of magnitude during a typical experiment, investigations of gases at extreme conditions are easily feasible from initial conditions at standard temperatures and pressures. Maximum temperatures and pressures above five thousand degrees Kelvin and five thousand atmospheres are easily achieved. Thus, ballistic piston compressors are ideal devices with which to study gases under extreme conditions of temperature and pressure.

Exact determination of the equation of state of the gas under investigation would necessitate continuous measurement of the temperature, pressure, and density of that gas. However, discrete measurement of these properties at even a selected part of the piston stroke provides enough information for the BCCC to analyze a substantial part of the equation of state. Thus, accurate information on the equation of state of a gas under investigation can be derived from measurements of the temperature, pressure, and density over part of the piston stroke. The best part of the stroke over which to obtain data is the end of the first compression stroke and the beginning of the first expansion stroke, thus including the maximum pressure and temperature, and the minimum volume. The measurements of these maxima and minima and their time relationships, in themselves, provide a wealth of information for analysis.

The experimental and analytical techniques developed in this report determine the thermodynamic parameters of the gas under consideration at high temperatures and pressures. To accurately describe the gas under consideration the Van der Waals' equation of state is used. One objective of these studies is the determination of the Van der Waals' constants a and b as functions of temperature. The ratio of the specific heats (i.e.,

constant volume and constant pressure) completes the thermodynamic parameters needed for gas description. Since the two specific heats are related, only one need to be analyzed by the system. The specific heat at constant volume has been selected.

Gas leakage past the piston, as shown later, is an important mechanism in ballistic piston compressors. In particular, the viscosity of the gas under test determines the leak rate. Since the leaking does not occur under conditions of streamline flow, the viscosity which determines gas leakage in a ballistic piston compressor will be a composite of the kinematic viscosity, dynamic viscosity, and associated turbulent effects. Dissociation is negligible for the temperature and pressures under consideration [4]. These facts must be considered when analyzing the measured viscosity.

II. EXPERIMENTAL APPARATUS

A. Ballistic Piston Compressor

The ballistic compressor used in the system is shown in Figure 1, and consists of four main parts, the reservoir, the piston release section, the tube, and the high pressure section. The compressor rests on five supports, the center three are steady rests, while the outer two consist of roller bearings. During assembly and alignment of the compressor all five supports are utilized. For firing, however, the three center supports are lowered and the compressor is then free to recoil on the two outer roller bearing supports without transmitting any force to the two tables. The two tables and the center support assembly are adjustable in height so that the compressor can be raised or lowered as necessary to align the radiation viewing window with the optical system.

The reservoir, shown in Figure 2, was designed for a maximum operating pressure of 136 atmospheres and was tested to 200 atmospheres. The testing and certification was made by a separate concern from the one that fabricated the reservoir. With this reservoir it is possible to generate a 10,000 atmosphere test gas pressure for any test gas with an initial pressure of up to two atmospheres. The volume of the reservoir is about 60 liters, sufficiently large that the driver gas pressure does not drop excessively as the piston travels down the barrel.

The piston release section serves two functions: it fires the piston and in addition makes possible the sealing off of the reservoir

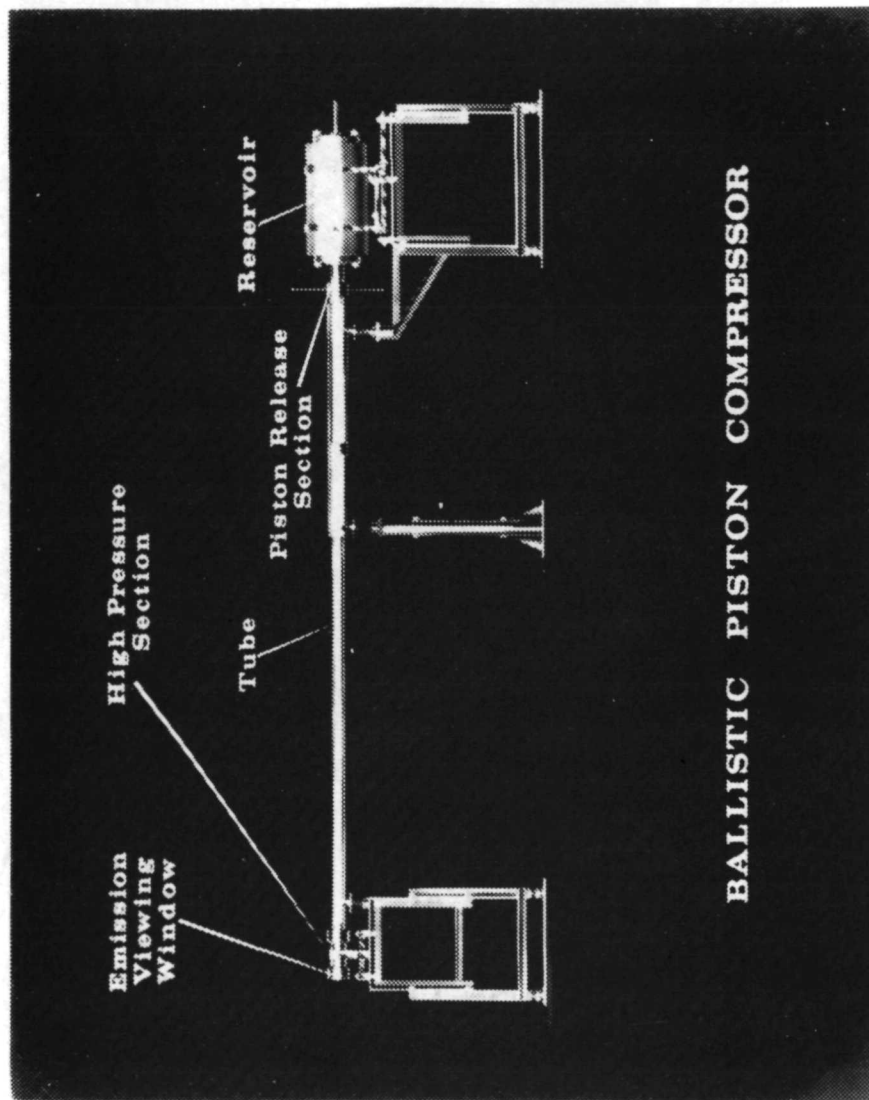


FIGURE 1. BALLISTIC PISTON COMPRESSOR

PARCHMENT DEED

SOUTHWOOD CO. U.S.A.
100% COTTON FIBER

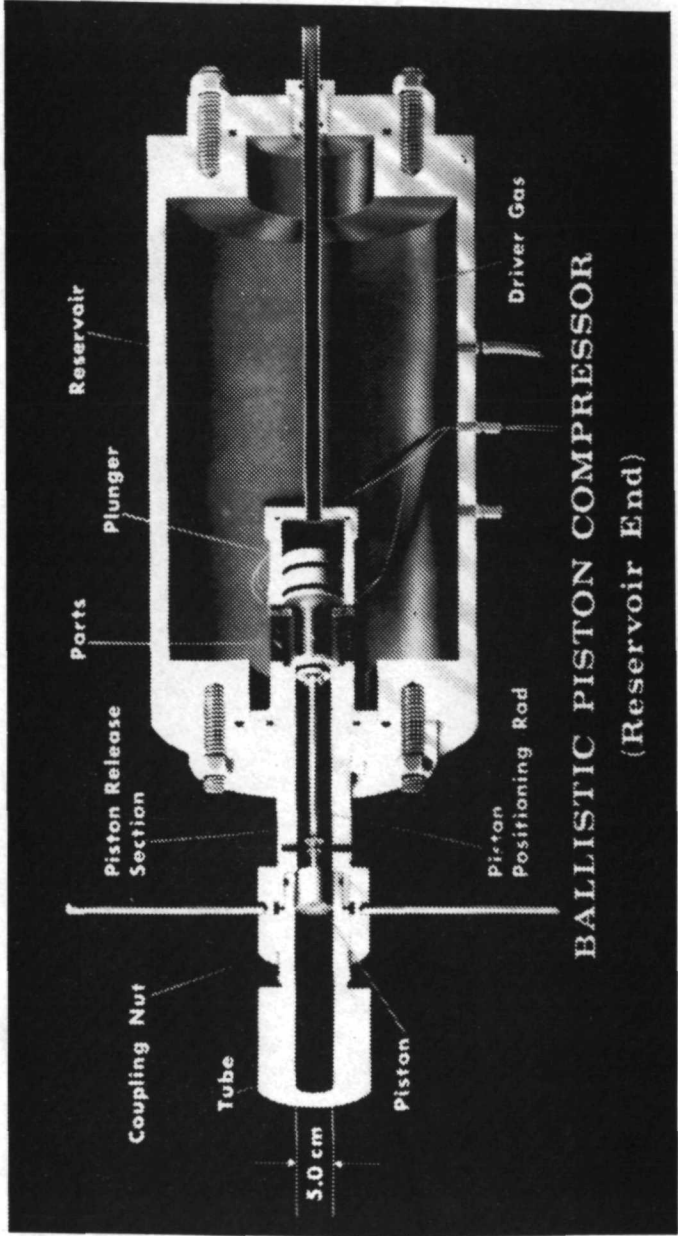


FIGURE 2. BALLISTIC PISTON COMPRESSOR (RESERVOIR END)

gas from the tube in such a manner that the tube and high pressure section can be disassembled safely while the reservoir is fully charged with driver gas pressure. This feature greatly facilitates the experimental work, since it makes possible the exchange of pistons, windows, and pressure gauges, and allows inspection of the barrel bore and high pressure section, without time consuming and expensive dumping of the reservoir pressure.

Figure 2 shows the piston release section in position between the tube and reservoir. It consists of a cylinder closed on one end with a cap to which is welded a length of pipe. This pipe goes through the wall of the reservoir to the gas supply system. Four ports are located in the walls in the front part of the cylinder. The two ends of the plunger when located in the front part of the cylinder bridge the four ports. The plunger necks down from a 7.61 cm diameter on the reservoir side to a 4.44 cm diameter on the barrel side. The large diameter part of the plunger contains two neoprene O-rings while the small diameter part contains one. In moving to the rear position the plunger fires the piston. A safety cap is screwed onto the barrel end of the piston release section whenever the barrel or high pressure section is disassembled while the reservoir is charged with driver gas pressure. An accidental loss of gas pressure behind the plunger, releasing the driver gas, would thus not endanger personnel or equipment.

The barrel is 3.89 meters long and has a 0.09 mm bore. The material is A.1.S.1 4340 steel with a yield strength of 12,650 Kg/cm²; the hardness is Rockwell C 42-45. The 50 mm bore section is 17.78 cm long; the wall thickness is 2.57 cm. A gas inlet is located in the wall to facilitate

movement of the piston while checking the apparatus. This section was designed for pressures up to 5,000 atmospheres. Since the high temperatures which are generated in the high pressure section shown in Figure 3 cause a slight vaporization of the inner walls with the resulting emission of unwanted impurity radiation, the inner bore was plated with chromium.

Figure 4 shows the piston and cup seals in detail. To minimize gas leakage around the piston, two cup seals are employed. The gases before and behind the piston expand these seals against the bore thus minimizing gas leakage around the piston. The piston body is made of steel. Two phosphor bronze bearings provide the surface upon which the piston moves. The head of the piston is made of molybdenum to prevent ablation by the hot gas.

The gas handling system is shown in Figure 5. Most of this system is housed in a mobile control console. This console controls the test gas and reservoir fill pressures. It also contains the vacuum system and helium purification system. Firing and post-firing procedures are implemented from this console. A relationship between the reservoir pressure and the maximum pressure of the test gas can be easily derived. This is accomplished by equating the work done by the reservoir gas done by the piston to the work done by the piston on the test gas. The assumptions for this derivation are

- 1) ideal test gas
- 2) no gas leakage across piston
- 3) adiabatic process
- 4) constant reservoir pressure

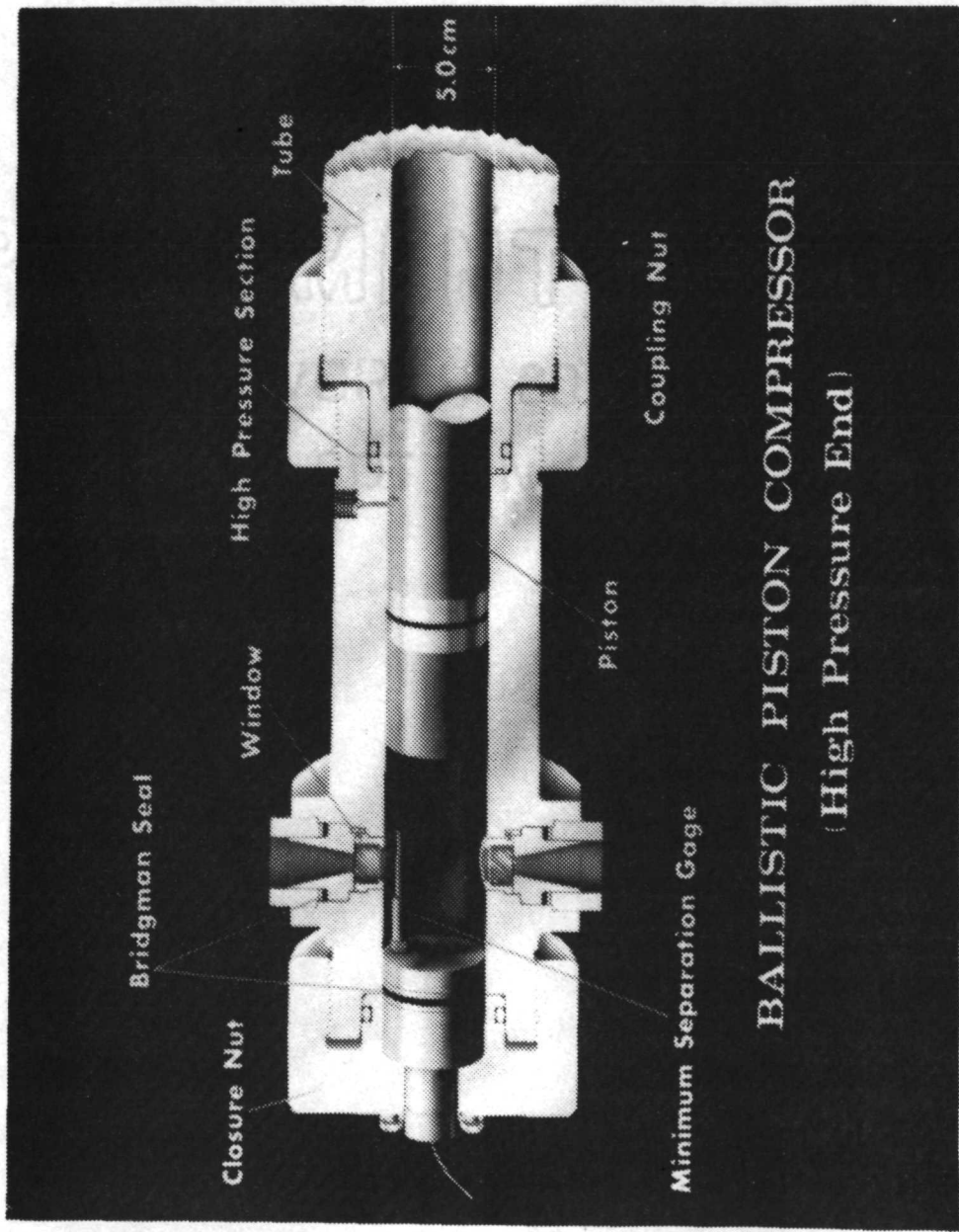


FIGURE 3. BALLISTIC PISTON COMPRESSOR (HIGH PRESSURE END)

PARCHMENT DEED
SOUTHWORTH CO. U.S.A.
100% COTTON FIBRE

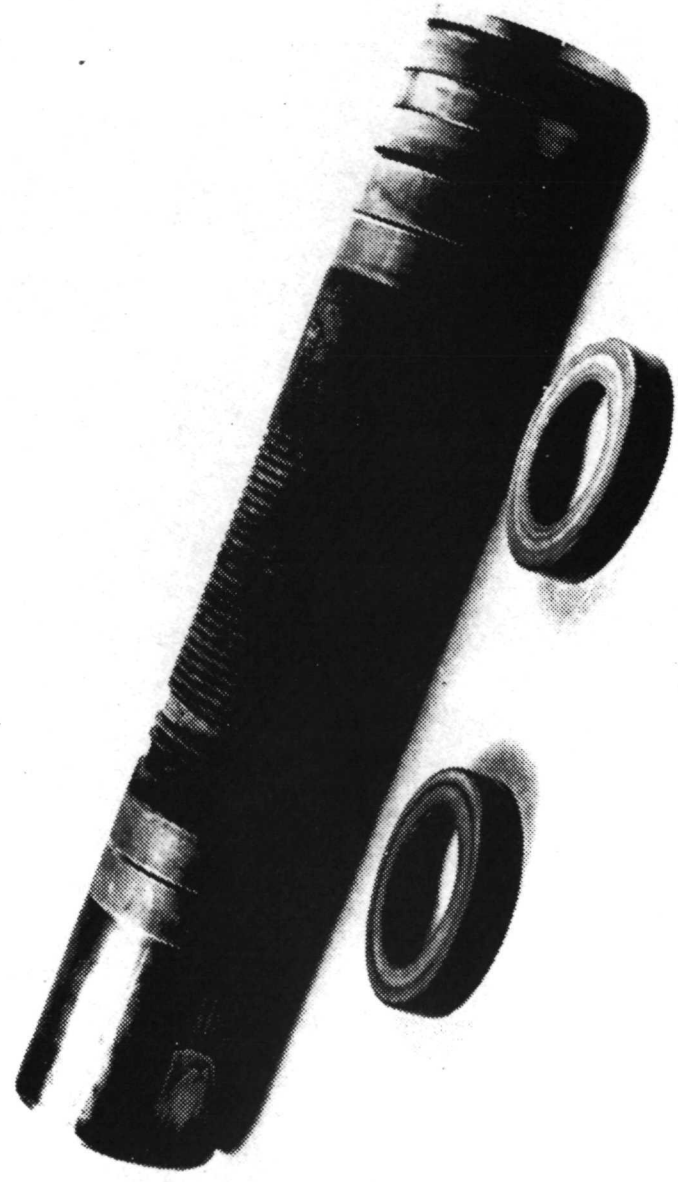


FIGURE 4. PISTON AND CUP SEALS

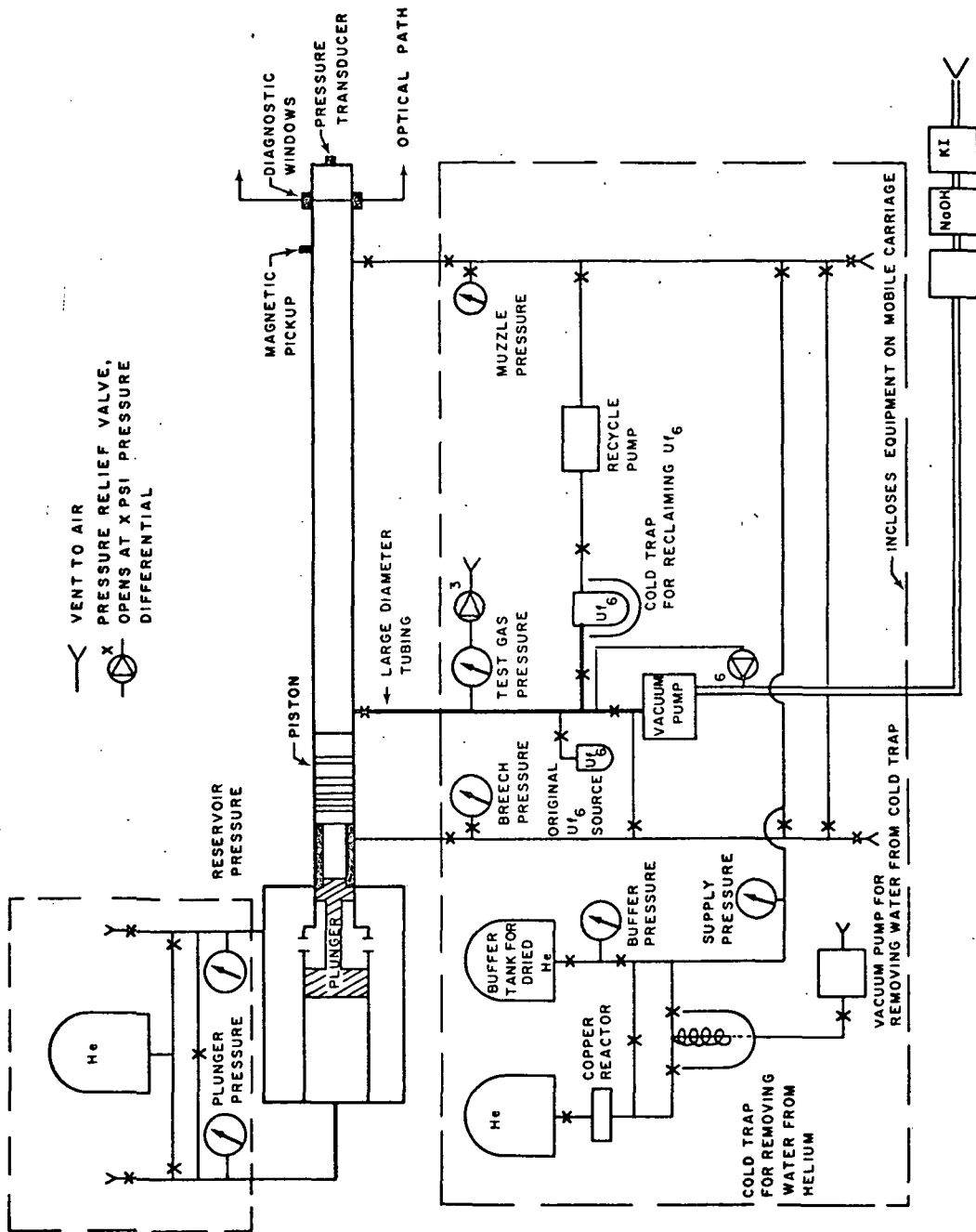


FIGURE 5. GAS HANDLING SYSTEM

This gives the following equation

$$\frac{P_{res}}{P_0} = \frac{\frac{P_{max}}{P_0} - \left(\frac{P_{max}}{P_0}\right)^{1/\gamma}}{\left(\frac{P_{max}}{P_0}\right)^{1/\gamma} - 1} \quad (1)$$

This equation shows that large values of maximum test gas pressures can be obtained for relatively modest reservoir pressures.

B. Diagnostics

1. Measurement of Test Gas Pressure

The data acquisition system is shown in Figure 6. Possible optical misalignment caused by compressor recoil is monitored by means of a slidewire resistor, sensing the position of the high pressure test section.

The pressure of the test gas is measured continuously with a calibrated Kistler pressure transducer. A charge amplifier provides bias to the transducer. The oscilloscope trace of the output of the pressure transducer is photographically registered. The charge amplifier also provides a calibration signal for the range of interest, as well as a zero pressure reference. Both of these traces are photographed before each experiment. Figure 7 shows the results of a typical pressure measurement showing the pressure signal, the 5000 psi calibration trace, and the zero baseline trace.

2. Measurement of UF₆ Pressure

The pressure of the uranium hexafluoride is measured with a Wallace and Tiernan model FA160 absolute pressure gauge. Initially the test section is evacuated and then filled to the appropriate pressure of uranium hexafluoride.

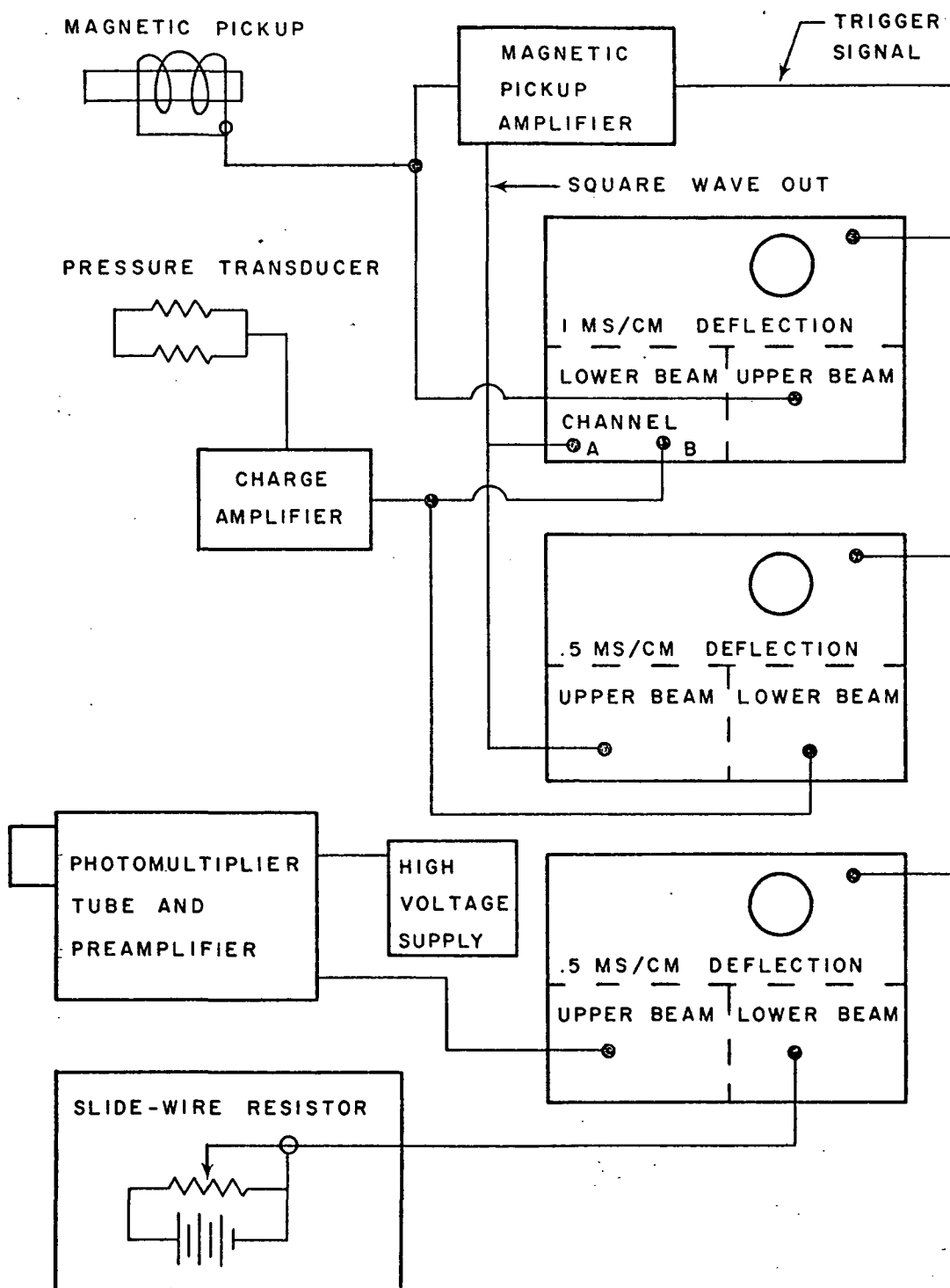
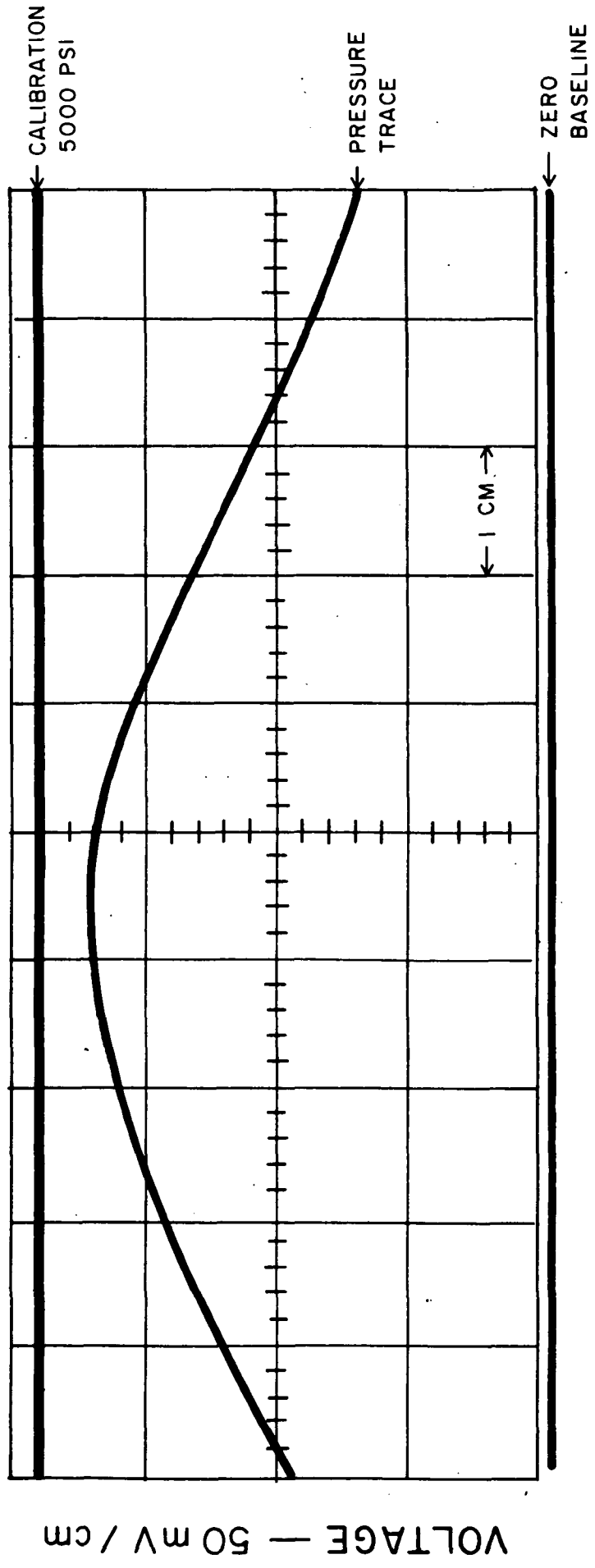


FIGURE 6.

DATA ACQUISITION SYSTEM



TIME — 0.5 msec / cm

FIGURE 7. BASELINE, CALIBRATION, AND PRESSURE TRACES

The gas line from the uranium bottle to the compressor barrel consists of twenty inches of quarter inch copper tubing followed by four feet of one inch flexible tubing leading to the barrel. There is a quarter inch port (or "touch-hole") drilled in the barrel, just ahead of the initial piston position, to which the flexible tubing is connected.

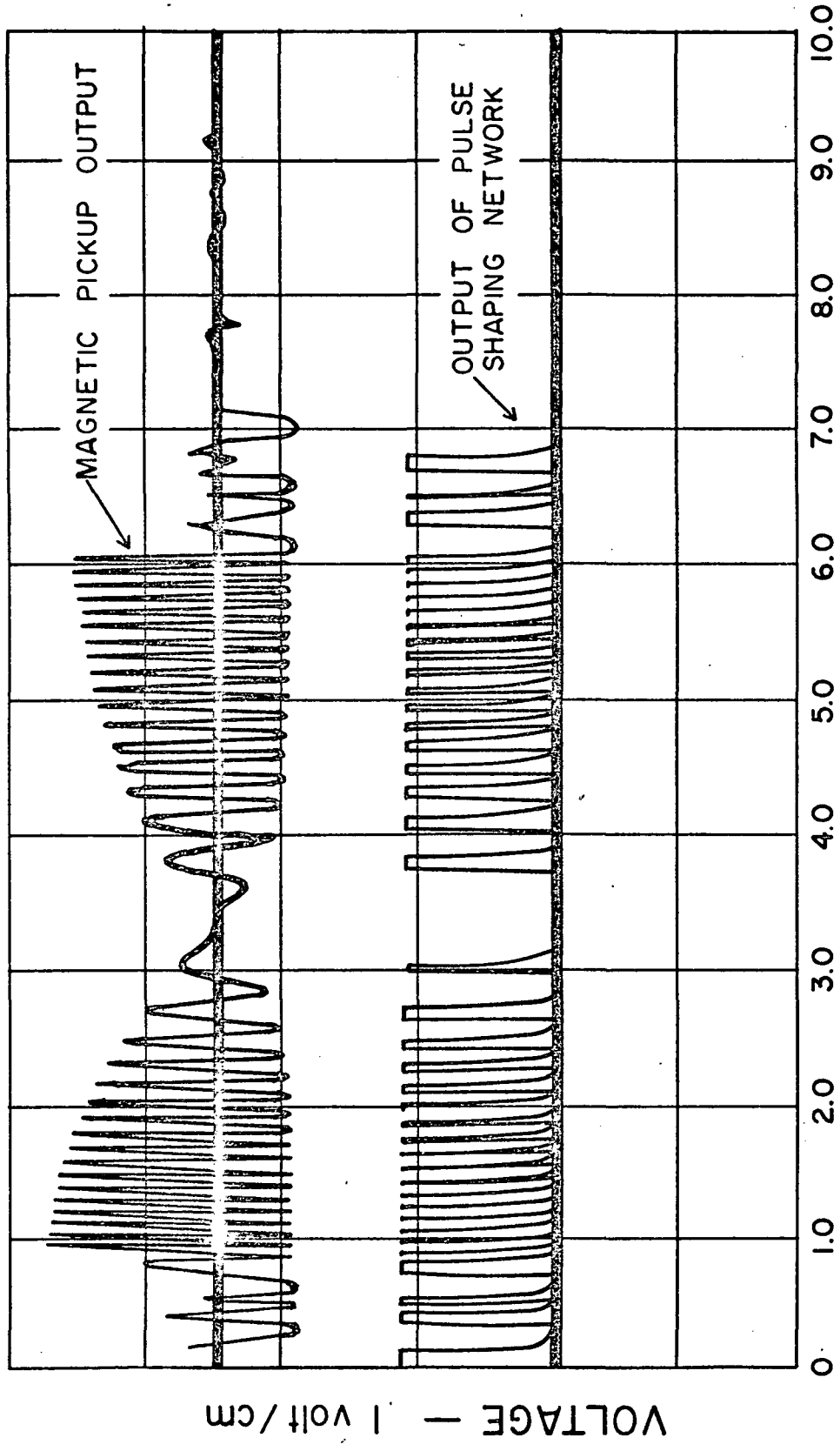
The tap to the absolute pressure gauge consists of three feet of quarter inch copper tubing which is connected to the flexible tubing. After each filling of the barrel and test section, but before each reading of the uranium hexafluoride pressure, at least five minutes were allowed for equilibrium to be established.

After filling with uranium hexafluoride, the test section is filled with helium to a total pressure of one atmosphere. The total pressure is determined with a differential pressure gauge.

3. Volume Measurement

To measure the volume of the test gas mixture near maximum pressure, the high pressure test section is instrumented with a magnetic pickup, which senses the position of the piston during compression [5].

The body of the piston has circumferential grooves at measured distances. The voltage signal induced in the magnetic pickup by these grooves is applied to a pulse shaping network which produces a square wave for each groove which passes the magnetic pickup. The return of this square wave to baseline coincides with the middle of the associated "tooth". Figure 8 shows the voltage signal from the magnetic pickup and the associated square waves. The square wave generator also provides a radio frequency triggering signal beginning with the first groove. This signal is used to trigger the data acquisition system. Figure 9 illustrates the geometric configurations of the piston and magnetic pickup.



TIME — MILLISECONDS

FIGURE 8. TRACE OF MAGNETIC PICKUP AND AMPLIFIER OUTPUT

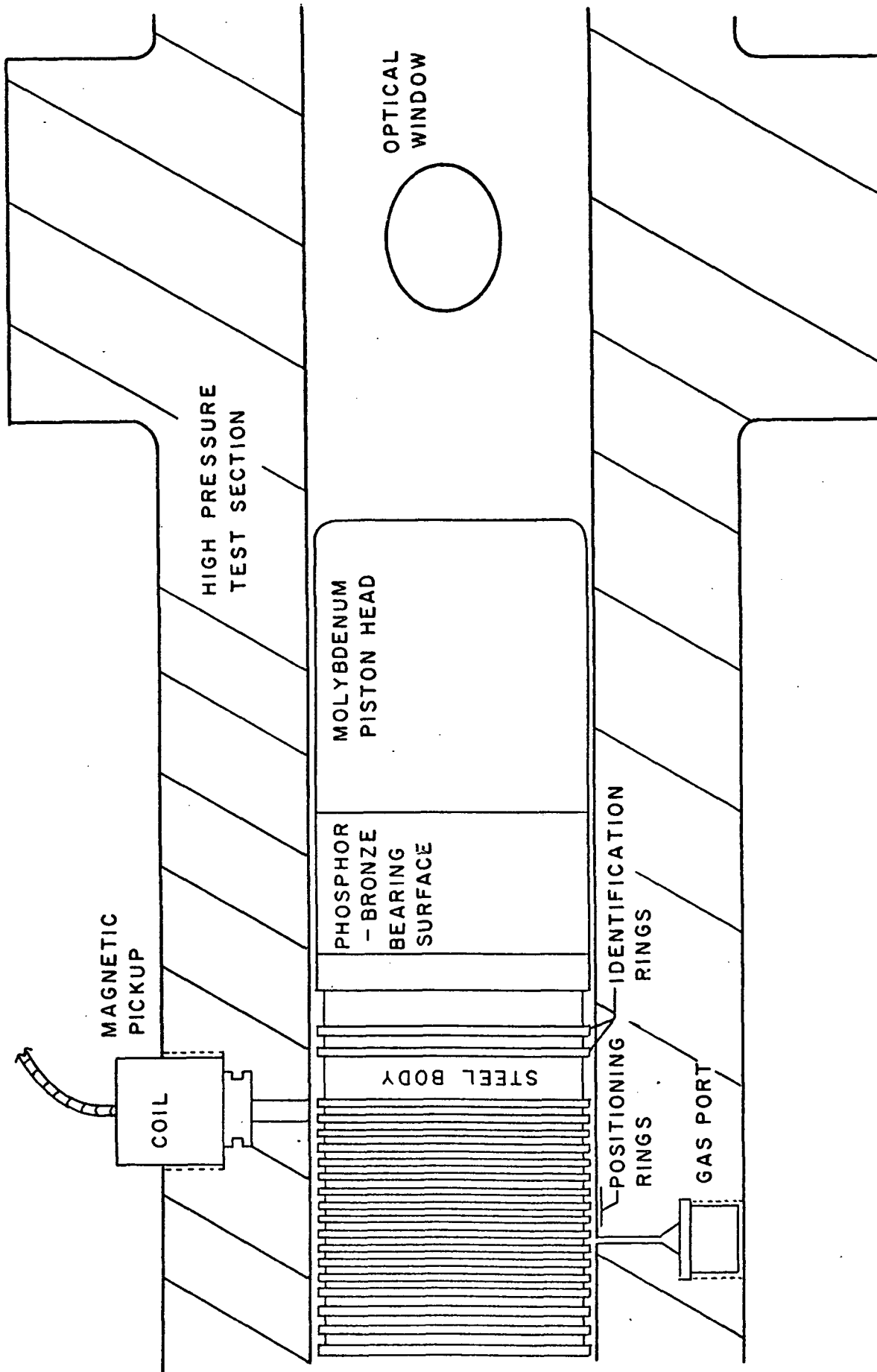


FIGURE 9.
DIAGRAM ILLUSTRATING MAGNETIC PICKUP

4. Temperature Measurement

The temperature of the test gas is measured by the brightness-emissivity method. In this technique the emission and absorption of the gases are measured and the ratio of these values is used to determine the temperature of the test gas.

Ideally the emission and absorption should be measured simultaneously. However, they can be measured alternately if conditions in the test gas do not change appreciably between measurements. The latter method is used as shown in Figure 10.

Because of the relatively low temperature of the test gas, the helium is not sufficiently excited to allow the measurement of temperature to be made on a spectrum line of helium. Therefore a small amount of NaCl is introduced into the high pressure test section. The temperature is measured using the 589nm sodium line.

The He-Na collision cross section is sufficiently large that approximate equilibrium is set up between the temperatures of the helium and sodium atoms despite the low electron density.

The temperature of the test gas is given by:

$$1/T = 1/T_L + k/h\nu \ln\left(1 + \frac{V_2 - V_3}{V_1}\right) \quad (2)$$

where the following symbols have been used:

- k the Boltzmann constant
- h the Planck constant
- ν the central frequency of the sodium line
- T_L the brightness temperature of the standard lamp
- V_1 the photomultiplier output voltage when the standard lamp is cut off by the rotating disk,

and hence corresponds to the intensity of the radiating sodium line

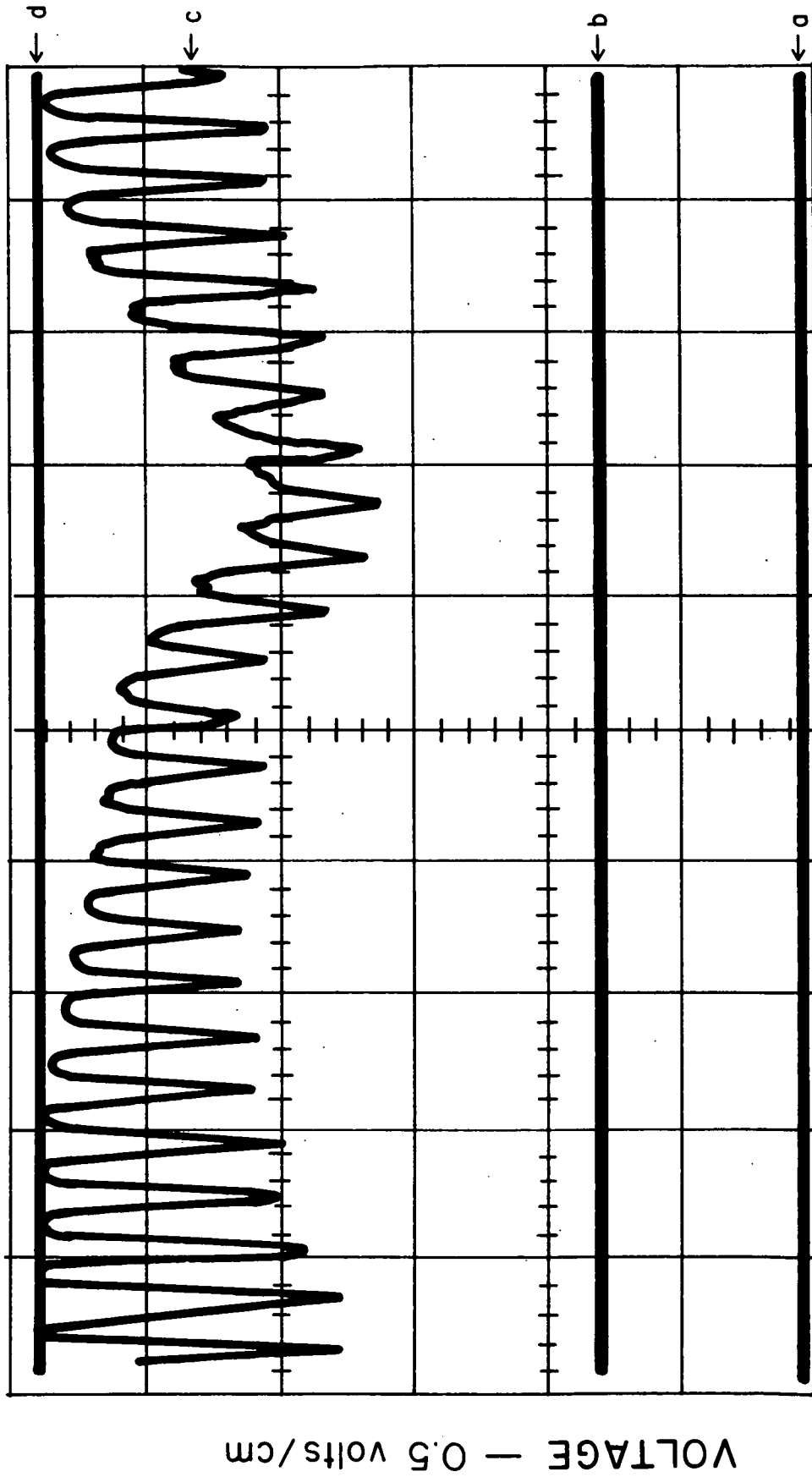
- V_2 the voltage of the photomultiplier when only the standard lamp is emitting (i.e., with a cold plasma)
- V_3 the voltage of the photomultiplier with standard lamp and emitting test gas

A tungsten standard lamp is used. The lamp temperature is adjusted to be close to the temperature expected in the test gas. Figure 10 shows the trace of the raw data of a typical temperature measurement.

The validity of the above method hinges on the assumption of thermodynamic equilibrium of the system. Since the velocity of the piston is on the order of a tenth of the speed of sound, it is reasonable to assume that the gas is in thermodynamic equilibrium.

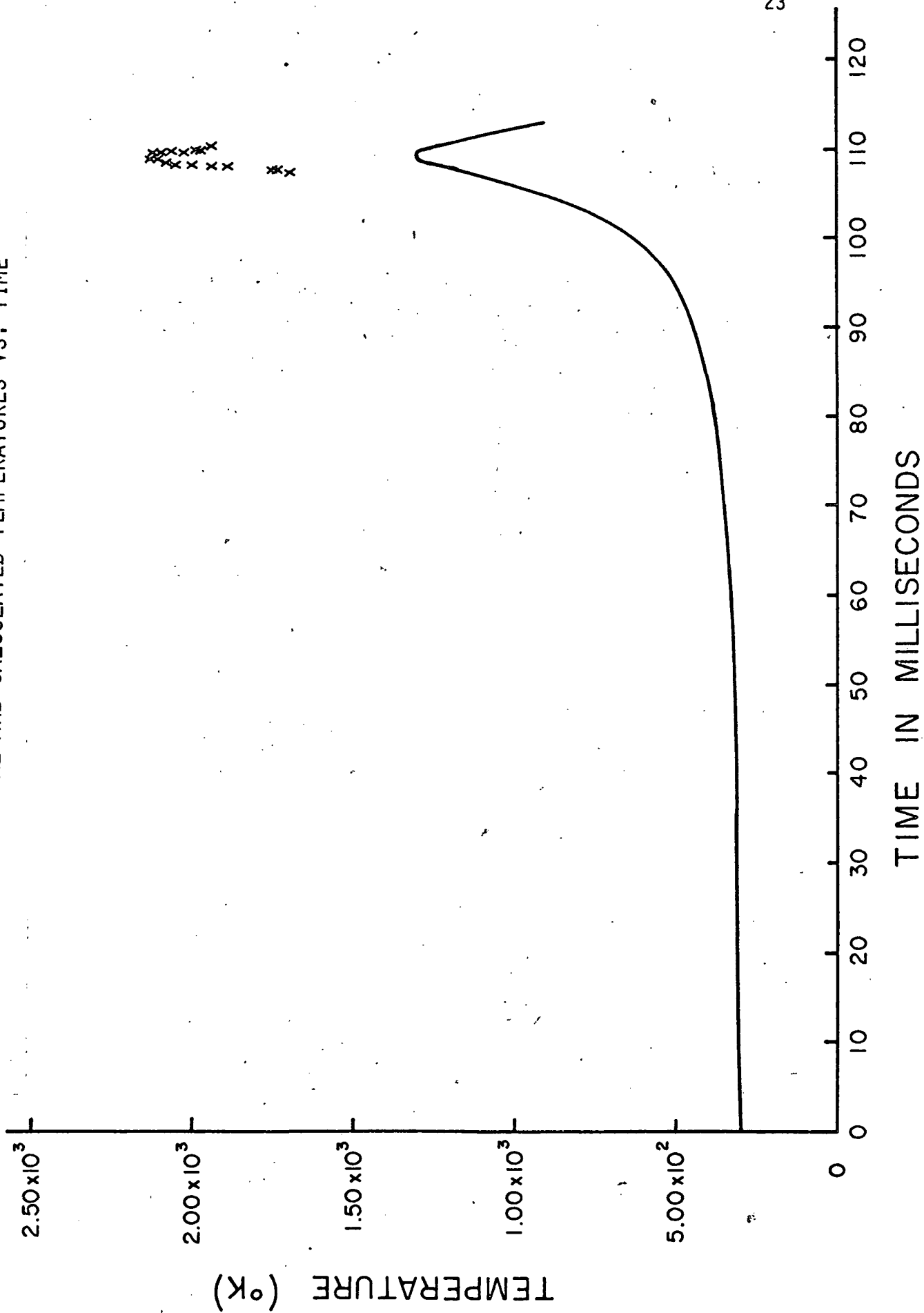
Only the center portion of the pressure broadened sodium doublet was used for these measurements. This ensures that a high signal to background (continuum) ratio was achieved. Figure 11 shows the results of the temperature measurements using the brightness emissivity method compared to the temperatures computed by the BCCC. The measured values are higher than the computed values by about 25%, which is consistent with previously reported results [6].

FIGURE 10. RAW DATA OF BRIGHTNESS EMISSIVITY TEMPERATURE MEASUREMENT



- a. RELATIVE POSITION OF BARREL BEFORE FIRING
- b. RELATIVE POSITION OF BARREL DURING FIRING
- c. BRIGHTNESS EMISSIVITY METHOD
- d. O-REFERENCE VOLTAGE FOR BRIGHTNESS EMISSIVITY METHOD

FIGURE 11. EXPERIMENTAL AND CALCULATED TEMPERATURES VS. TIME



III. THEORETICAL REVIEW

A review of the theory employed in obtaining the numerical algorithms used in the BCCC (Ballistic Compressor Computer Code) is presented. The Van der Waals' equation of state and the expression for the specific heat ratios derived from that equation of state provide introduction for their subsequent use in slightly modified form.

Non-ideal processes are examined and reference is made to analytical evidence suggesting that such processes cannot be neglected. The rate equations for gas leakage and heat loss complete the analytic expressions of primary interest.

The numerical equivalent of the heat equation for the cylindrical bore introduces similar equations in the following chapter. The expression for the work done on the piston by the leaking gas and an empirical formula for the viscosity complete this chapter.

A. Equation of State

The Van der Waals' equation of state is:

$$(p + a/v^2)(v - b) = RT \quad (3)$$

where a and b are the Van der Waals' constants. In general a and b are functions of temperature, and are represented by a second degree polynomial in temperature:

$$a = a_1 + a_2T + a_3T^2 \quad (4)$$

$$b = b_1 + b_2T + b_3T^2 \quad (5)$$

Theoretical temperature independent values may be obtained for a and b from "real gas" theory [6]:

$$a = 3p_c v_c^2 \quad (6)$$

$$b = v_c/3. \quad (7)$$

p_c and v_c are respectively, the critical pressure and the critical molar volume. Table 2 lists the Van der Waals' constants for helium; the values for uranium hexafluoride are calculated from its triple point.

B. Specific Heat Ratios

One of the principal objectives of this investigation is the determination of the ratio of specific heats of uranium hexafluoride. The specific heat ratio or "gamma" as it is sometimes referred to given by:

$$\gamma = 1 + \frac{R}{C_v} \frac{pv^3 + av}{pv^3 + av - 2a(v-b)} \quad (8)$$

where C_v is the specific heat of the gas at constant volume. In general this parameter is a function of temperature. For the uranium hexafluoride, a second degree polynomial representation in temperature is made of C_v . The specific heat of helium is assumed to be constant over the range of conditions to be investigated.

C. Non-Adiabaticity of the Compression Process

Ideally, the ratio of specific heats would be measured in a polytropic process. That is, the pressure, temperature or volume of the gas of interest would be measured as the gas is compressed without loss of heat or mass. These conditions are approached in the rapid compression

Table 2

Van der Waals' Constant of He and UF₆

UNITS	$\frac{\text{atm}}{(\text{L/mole})^2}$	$\frac{\text{atm}}{(\text{L/mole})^2 \cdot \text{K}}$	$\frac{\text{atm}}{(\text{L/mole})^2 \cdot \text{K}^2}$	L/mole	L/mole-°K	L/mole-°K ²
	a ₁	a ₂	a ₃	b ₁	b ₂	b ₃
He	0.120	-5.75×10^{-3}	7.68×10^{-8}	.0116	-8.72×10^{-6}	1.94×10^{-9}
UF ₆	8.95	-	-	0.082	-	-

of a gas by a piston. However, it has been shown [2] that while a gas is compressed by a ballistic piston, heat is lost to the barrel walls and gas is lost past the piston. Additionally, it would be expected in the ideal compression of a gas, that the maximum pressure and minimum volume would occur simultaneously. Results show they do not. As shown in Figure 12, the minimum volume may occur after the maximum pressure by as much as a millisecond. This phenomenon is caused by leakage of the test gas past the piston. It has been estimated that the leakage rate is on the order of ten moles of test gas per second at the point of maximum compression [2]. Clearly, this represents a significant departure from the ideal compression of a known amount of gas.

The amount of heat lost from the test gas during the compression process is also significant. This non-adiabaticity may be examined by comparing the heat conducted through the wall to the heat necessary to raise the temperature of the gas during the compression stroke [2].

To assume adiabatic compression, the following inequality must hold:

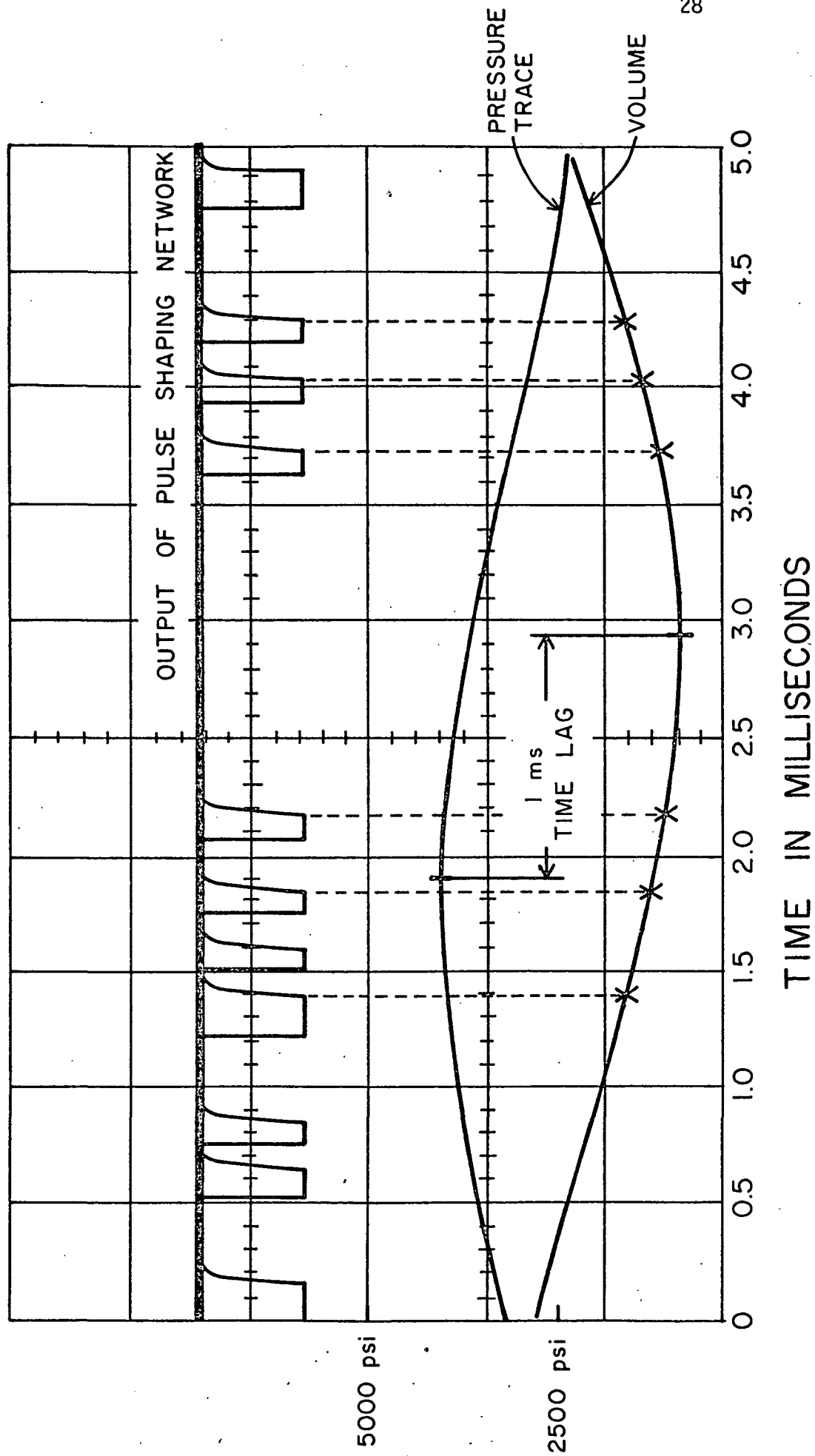
$$dQ_{\text{lost}} \ll MC_V \Delta T \quad (9)$$

The right hand side of this equation is the heat necessary to raise the temperature of the test gas by ΔT . After solving for the motion of the piston, the above inequality gives the relation [2]:

$$\frac{2\pi K(X_0 - X)^2 \left[1 - \left(\frac{X_0 - X}{X_0}\right)^{\gamma-1}\right]}{M C_V \ln(1 + \alpha/\gamma_0)} \ll (\gamma-1) \sqrt{AP_{r0}/m} (X/X_0)^{1/2} \sum_n \alpha_n (X/X_0)^n \quad (10)$$

FIGURE 12.

TIME COMPARISON OF MINIMUM VOLUME & MAXIMUM PRESSURE



where the following symbols have been used:

K	the thermal conductivity of the barrel wall (steel)
X_0	the initial length of the test gas section
X	length of tube occupied by the test gas
γ	specific heat ratio (for this equation the test gas is the same as the reservoir gas)
M	mass of the test gas
C_v	specific heat of the test or reservoir gas
α	cylinder wall thickness
r_0	radius of inner barrel surface
P_{r0}	initial pressure of the reservoir gas
m	mass of the piston
α_n	coefficients of the power series resulting from the solution for the velocity of the piston
A	cross sectional area of the piston

The non-adiabaticity of the compression process is illustrated by considering the end of the first piston stroke where the piston's velocity is nearly zero. This is where the test gas temperature exceeds room temperature by the greatest amount. It has been shown [2] that in this region the right hand side has a value of nearly zero while the left hand side has a value of about five. Thus, the above inequality is not satisfied and the process cannot be assumed to be adiabatic.

The other significant departure from an ideal process is the mixing of the test and reservoir gases. This mixing is the result of leakage due to the pressure difference between both ends of the piston as well

as to the motion of the piston. The leaking rate is related to the viscosity of the leaking gas by the equation [2]:

$$dn/dt = \frac{\pi \rho}{m_a} r_o (r_o - r_p) \left[\frac{1}{8\eta} \frac{\partial P'}{\partial X} (r_o - r_p)^2 + V \right] \quad (11)$$

where the following symbols have been used:

dn/dt	leaking rate
ρ	density of the leaking gas
m_a	molecular weight of the leaking gas
r_o	inner radius of the barrel
r_p	radius of the piston
η	viscosity of the leaking gas
V	piston velocity
$\partial P'/\partial X$	the pressure gradient along the piston

The quantity $(r_o - r_p)$ is also known as the piston gap and, as the term implies is the clearance separating the piston and tube wall.

Heat loss from the test gas to the bore wall must be calculated numerically and the energy thus lost must be subtracted from the internal energy of the test gas mixture. In cylindrical coordinates, the heat equation is:

$$\frac{\partial T}{\partial t} = \alpha \left(\frac{\partial^2 T}{\partial r^2} + \frac{1}{r} \frac{\partial T}{\partial r} \right) \quad (12)$$

where α is the thermal diffusivity of the steel barrel. For numerical purposes, the bore thickness is divided up into nodes, and the temperature at each node is calculated. Let the subscript i denote the i th iteration in time, and the subscript j denote the node at radius

$[R_{inner} + \Delta r]$:

$$\frac{T_{i+1,j} - T_{i,j}}{\Delta t} = \alpha \left(\frac{T_{i,j+1} - 2T_{i,j} + T_{i,j-1}}{\Delta r^2} \right) + \frac{1}{R_{\text{inner}} + j\Delta r} \left(\frac{T_{i,j+1} - T_{i,j-1}}{2\Delta r} \right) \quad (13)$$

where R_{inner} is the inner radius of the bore. The new temperature at time step $i+1$ and node j becomes:

$$T_{i+1,j} = T_{i,j+1} \left(\frac{1}{\Delta r^2} + \frac{1}{2(R+j\Delta r)\Delta r} \right) \alpha \Delta t + T_{i,j} \left(1 - \frac{2\alpha \Delta t}{\Delta r^2} \right) + T_{i,j-1} \left(\frac{1}{\Delta r^2} - \frac{1}{2(R+i\Delta r)\Delta r} \right) \alpha \Delta t \quad (14)$$

where Δt is the width of the current time step.

The work done by the leaking gas on the piston is given by:

$$E = \frac{2RL_p V \eta}{G} \pi \Delta X - (P_r - P) G r \pi \Delta X \quad (15)$$

where L_p is the length of the piston and G is the piston gap.

The above expressions are implemented numerically to simulate a ballistic piston compressor. By taking short time steps (i.e., one microsecond), the motion of the piston may be calculated and the changing thermodynamic conditions monitored. That is, as the piston "steps" down the tube numerically, the changing velocity, temperature, and pressure, etc., may be accurately followed.

Since several parameters needed at each time step change with temperature, etc., they must be recalculated. Included is the specific heat at constant volume of the UF_6 and the Van der Waals' constants. Others must be recalculated as the ratio of UF_6/He changes due to gas leakage. In fact, the characteristics of the test gas mixture may change dramatically due to helium leaking into the test gas at the beginning of

the compression stroke. Therefore, the thermodynamic parameters of the test mixture must be re-evaluated at each time step.

An empirical formula has been used to describe the change in the viscosities of the gas as a function of temperature:

$$\eta = AT^B \quad (16)$$

A and B are also assumed to be linear functions in temperature:

$$\eta = (A_1 + A_2T)T^{B_1+B_2T} \quad (17)$$

Using this equation, the viscosity is also recomputed each time step.

IV. ANALYTICAL TECHNIQUE

Implementation of the theory is achieved by means of a numerical scheme to simulate the motion of the piston in a ballistic piston compressor. In this scheme, the movement of the piston is divided into steps and at every step, the nonlinearities are approximated and introduced into the equations of state. The final result of the simulation is a tabulation of the variables of interest as a function of time. In general the outputted variables include the length of bore occupied by the test gas, the ratio of specific heats of the test gas, the pressure, temperature, number of moles of the test gas mixture, the pressure of the reservoir, and the acceleration of the piston.

The numerical and experimental data are then aligned in time and errors are assigned to the numerical data. By taking the partial derivatives of the errors with respect to those thermodynamic parameters being optimized a quantitative measure is obtained of how to adjust those thermodynamic parameters to reduce the error. When the error becomes insignificant, those thermodynamic parameters which accurately describe the gas have been found.

A. Piston Motion Simulation

The program developed to analyze the piston motion in a ballistic piston compressor models the first compression and expansion stroke of the compressor under analysis. As explained previously, there are several nonlinear processes which must be included in any accurate analysis.

The first requirement for the program then, is that its time step must be small enough to give adequate treatment to the nonlinearities such as gas leakage and heat loss.

Each time step calculates piston movement, heat loss to the cylinder walls, gas leakage past the piston, and work done on the piston. In addition, since a test gas mixture of two species is to be analyzed, and since the proportions of the mixture may change with leakage, each time step must recalculate thermodynamic parameters of the test gas mixture. Figure 13 gives the flow chart of the simulation part of the BCCC.

Each time step is begun by calculating piston displacement from the velocity and the width of that time step.

$$\Delta X = V\Delta t \quad (18)$$

where X is the length of bore occupied by the test gas and V is the velocity of the piston. New temperatures and pressures are calculated on the basis of this change in volume:

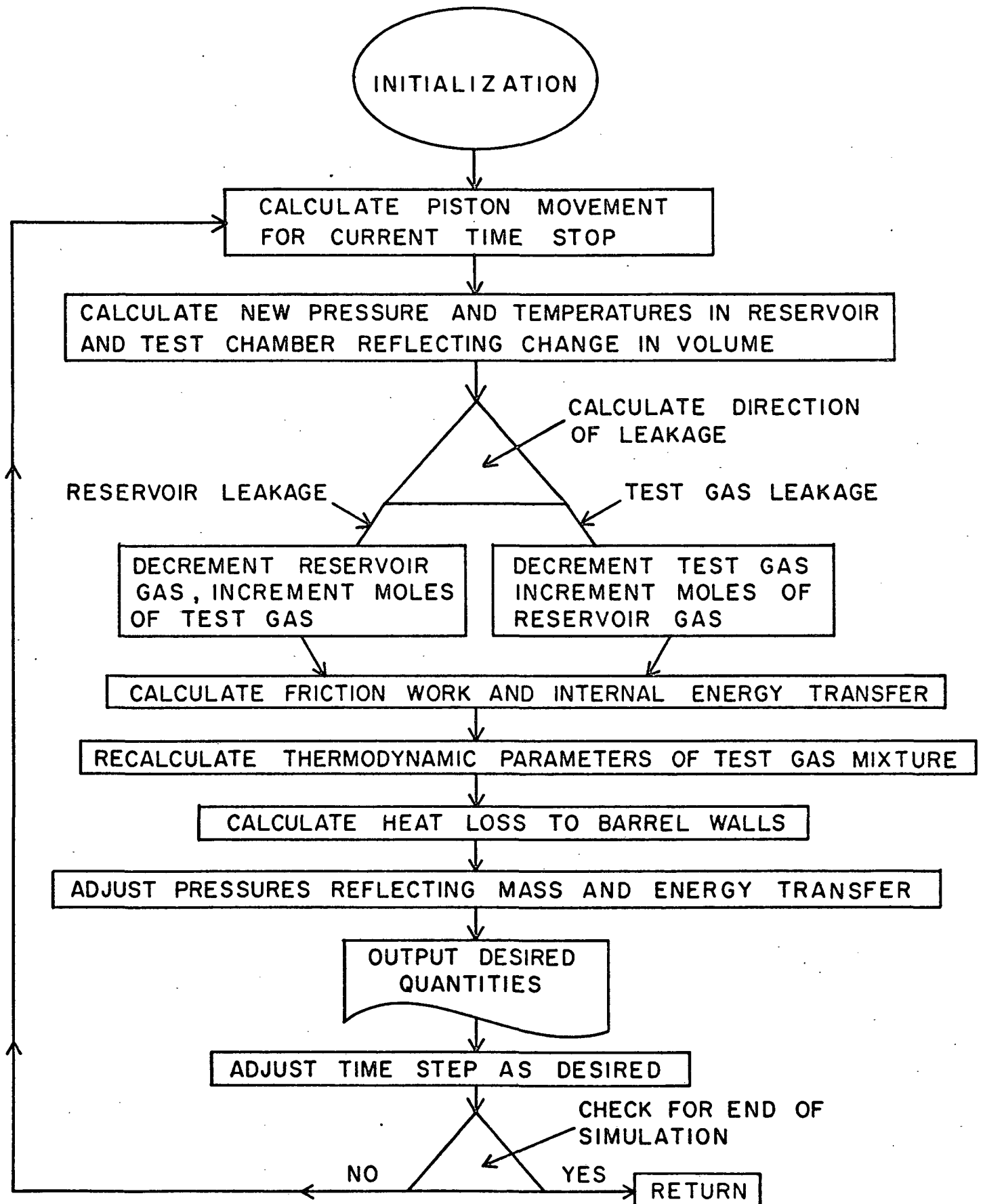
$$P_i = \left(P_{i-1} + \frac{a}{V^2}\right) \left(1.0 \pm \frac{\Delta V}{V-b}\right)^{-\gamma} \frac{2a(V-b)}{[(PV^2+a)(V\pm\Delta V)-2a(V-b)]C_v} - \frac{a}{(V\pm\Delta V)^2} \quad (19)$$

$$T_i = \frac{(V\pm\Delta V-b) \left(P_{i-1} + \frac{a}{V^2}\right) \left(1.0 \pm \frac{\Delta V}{V-b}\right)^{-\gamma} \frac{2a(V-b)}{[(PV^2+a)(V\pm\Delta V)-2a(V-b)]C_v}}{R \cdot n} \quad (20)$$

P_i new pressure of current time step

P_{i-1} pressure of previous time step

FLOW CHART OF BCCC SIMULATOR



- a Van der Waals' constant multiplied by the number of moles of gas squared
- b Van der Waals' constant multiplied by the number of moles under consideration
- V reservoir or test volume under consideration
- γ specific heat ratios of gas under consideration
- C_v specific heat of gas under consideration
- R ideal gas constant
- n number of moles of test or reservoir gas under consideration
- \pm + for reservoir, - for test gas

Gas leakage past the piston is proportional to the pressure difference between the ends of the piston. Also the friction work of the leaking gas done on the piston is calculated at this time as well as the internal energy the leaking gas carries with it.

The sign of the pressure difference is tested to determine direction of leakage and then the number of moles leaked is calculated from:

$$\Delta m = \left(-\frac{(P_r - P)G^2}{8P_\ell \eta} + v \right) \frac{\pi r \Delta T}{v} G \quad (21)$$

The energy which the leaking gas carries with it is calculated by:

$$E_\ell = (TC_v + Pv)\Delta m \quad (22)$$

and the energy lost from the leaking chamber due to friction work is given by:

$$E_{fw} = \left[(P_r - P)rG - \frac{2RL_p V \eta}{G} \right] \pi \Delta x \quad (23)$$

These are used later in the time step to calculate pressure corrections in the reservoir and the test gas mixture.

With these pressures, temperatures, volumes, and gas leakage a new evaluation of the thermodynamic parameters of the test and reservoir gases is performed. This is necessary since the initial leakage of the reservoir gas into the test chamber can significantly alter the properties of the test gas. In the present case, the test gas is made up of helium and uranium hexafluoride. A numerical composite of the properties of these two gases is made at each time step.

Approximating the uranium hexafluoride-helium mixture by a single species test gas is done by weighing the thermodynamic parameters of each gas by the respective number density of that gas. By this method, the initial conditions of the single species is obtained, and those thermodynamic parameters which change during the compression or expansion of the test gas mixture are updated.

The number of moles in the single species approximation is equal to the sum of the moles of uranium hexafluoride and helium present.

Those parameters which are updated at each time step, during compression or expansion include the Van der Waals' constants, the specific heat at constant volume, and the viscosity. Also the number of moles of uranium hexafluoride and helium is updated at each iteration and the running totals are used in the update. When gas leaks into the test section from the reservoir side it is assumed that only helium has leaked into the test gas section and only the running total helium is updated. When gas leaks out of the test section, it is assumed that both helium and uranium hexafluoride have leaked out in proportion to their molar fractions present at the last time step. The relation used is:

$$n_{\text{UF}_6} = n_{\text{UF}_6}(\text{old})(1 + n_{(\text{lost})}/n_{\text{T}(\text{old})}) \quad (24)$$

$$n_{\text{He}} = n_{\text{He}}(\text{old})(1 + n_{\text{lost}}/n_{\text{T}(\text{old})}) \quad (25)$$

where $n(\text{old})$ indicates values from the previous time step, and $n_{(\text{lost})}$ is the number of moles leaked since the last time step. Since the optimization part of the BCCC assumes continuous parameters, the viscosity of the single species approximation of the test gas mixture is evaluated next. The viscosity coefficients "A" in equation 16 for the single species approximation are calculated from:

$$\begin{aligned} A_{1S} = & (n_{\text{He}}/n_{\text{T}})^2 A_{1\text{He}} + C_1 (n_{\text{He}} n_{\text{UF}_6} / n_{\text{T}}^2) \\ & + (n_{\text{UF}_6} / n_{\text{T}})^2 A_{1\text{UF}_6} \end{aligned} \quad (26)$$

$$\begin{aligned} A_{2S} = & (n_{\text{He}}/n_{\text{T}})^2 A_{2\text{He}} + C_2 (n_{\text{He}} n_{\text{UF}_6} / n_{\text{T}}^2) \\ & + (n_{\text{UF}_6} / n_{\text{T}})^2 A_{2\text{UF}_6} \end{aligned} \quad (27)$$

where the subscript "S" implies single species, n_{He} , n_{UF_6} , and n_{T} are respectively the number densities of helium, uranium hexafluoride, and the total of the two [8]. The variation of the exponent, B for the single species approximation is assumed to be the same as that of helium. The final result for the single species viscosity is then:

$$\eta_S = (A_{1S} + A_{2S}T)^{(B_{1\text{He}} + B_{2\text{He}}T)} \quad (28)$$

The specific heat at constant volume of the uranium hexafluoride is approximated as a function of temperature by:

$$C_V(\text{UF}_6) = C_1 + C_2T + C_3T^2 \quad (29)$$

The specific heat at constant volume of helium is assumed to be constant in those regions of interest. Table 3 gives the specific heat coefficients for helium and uranium hexafluoride. The specific heat at constant volume of the single species approximation is calculated by:

$$C_{VS} = \frac{n_{\text{He}}}{n_T} C_{V\text{He}} + \frac{n_{\text{UF}_6}}{n_T} C_{V\text{UF}_6} \quad (30)$$

Because the Van der Waals' constants of the helium and uranium hexafluoride cannot be combined in a simple relation to give coefficients of a single species, no updating is performed with respect to the mole fractions of helium and uranium hexafluoride on the Van der Waals' constants. The Van der Waals' constants of the single species approximation can initially be taken to be the same as those of helium, and then be optimized. Updating of the Van der Waals' constants is only done with respect to temperature. The relation used for the single species Van der Waals' constants are:

$$a_S = a_{1S} + a_{2S}T + a_{3S}T^2 \quad (31)$$

$$b_S = b_{1S} + b_{2S}T + b_{3S}T^2 \quad (32)$$

As demonstrated previously, the ratio of specific heats (equation 8) is a function of the specific heat at constant volume and the Van der Waals' constants. Since the Van der Waals' constants are not updated with respect to the mole fractions of the test gas, the ratio of specific heats is to a degree uncoupled from the changing mole fractions of the test gas mixture. However, this degree is small since the specific heat at constant volume is updated (both temperature and composition)

Table 3

Specific Heats at Constant Volume (C_V) of He and UF_6 Vapor

UNITS	(C_V/R)	$(C_V/R^\circ K)$	$(C_V/R^\circ K^2)$
	c_1	c_2	c_3
He	0.125	-	-
UF_6 [3]	1.140	8.21×10^{-4}	-

R--Ideal Gas Constant

and its effect on the ratio of specific heats is much greater.

Heat loss to the bore walls and end plugs (one of which is the piston) is calculated each time step. The thicknesses of the cylinder walls and end plugs are divided up into nodal points at which the temperature is evaluated. At most, a hundred nodes are used for either the cylinder walls or end plugs. The end plugs are assumed to be twice as thick as the cylinder walls. The formulae used are:

$$\begin{aligned}
 T_{cj}(t_i) = & T_{c,j+1}(t_{i-1}) \left[\frac{1}{\Delta r^2} + \frac{1}{2(R+(j-1)\Delta r)\Delta r} \right] \alpha \Delta t \\
 & + T_{cj}(t_{i-1}) \left[1 - 2 \frac{\alpha \Delta t}{\Delta r^2} \right] \\
 & + T_{c,j-1}(t_{i-1}) \left[\frac{1}{\Delta r^2} - \frac{1}{2(R+(j-1)\Delta r)\Delta r} \right] \alpha \Delta t \quad (33)
 \end{aligned}$$

$$T_{c1}(t_i) = (T_{c2}(t_i) + H\Delta r T_{gas}(t_i)) / (1 + H\Delta r) \quad (34)$$

$$T_{cJ}(t_i) = T_{room} \quad (35)$$

where the subscript j is the nodal index, t_i is the i th time step, and T_c is the temperature of the cylinder wall.

For the end plugs, the formulae becomes:

$$\begin{aligned}
 T_{ej}(t_i) = & (T_{e,j+1}(t_{i-1}) + T_{e,j-1}(t_{i-1})) \frac{\alpha \Delta t}{(2\Delta r)^2} \\
 & + T_{ej}(t_{i-1}) \left(1 - 2 \frac{\alpha \Delta t}{(2\Delta r)^2} \right) \quad (36)
 \end{aligned}$$

$$T_{e1}(t_i) = T_{e2}(t_i) + H\Delta r T_{gas}(t_i) / (1 + H\Delta r) \quad (37)$$

The net heat flux into the test gas chamber is given by:

$$H_{in} = \left(\frac{2\pi r X k (T_{c2}(t_i) - T_{c2}(t_{i-1}))}{\Delta r} + 2AK \frac{(T_{e2}(t_i) - T_{e2}(t_{i-1}))}{2\Delta r} \right) \Delta t \quad (38)$$

The reservoir and test gas pressures are now adjusted to compensate for the heat flux out of the test gas, gas leakage, and work done on the piston:

$$P_{\text{new}} = P + (H_{\text{in}} - E_{\ell} + \{ \begin{matrix} E_{\text{fw}} \\ 0 \end{matrix} \}) R / (v-b) C_v \quad (39)$$

$$P_{\text{rnew}} = P_r + (E_{\ell} + \{ \begin{matrix} 0 \\ E_{\text{fw}} \end{matrix} \}) R / (v_r - b_r) C_{vr} \quad (40)$$

where the symbol $\{ \begin{matrix} \text{test gas leakage} \\ \text{reservoir leakage} \end{matrix} \}$ has been used to differentiate gas leakage between the two chambers.

The change in the velocity of the piston is now calculated from:

$$\Delta v = \frac{(P_r - P) A \Delta x + E_{\text{fw}}}{M_p V} \quad (41)$$

The change in the velocity of the piston concludes evaluation of physical parameters for the time step. The final computation of the time step concerns the width of the time step itself; whether it is to be increased, decreased, or remain the same. Two indicators are used in making this decision. They are the magnitude of the fractional change of velocity, i.e., $|(\Delta v / v)|$ and the fractional change in the pressure of the test gas mixture $(P(t_i) - P(t_{i-1})) / P(t_i)$. After consulting these indicators the time step is either increased by a factor of 1.2 or decreased by a factor of 0.8 or remains the same.

Also at this point output of the time step is performed. Output variables of interest may include the time, pressures, temperatures, thermodynamic parameters, etc.

Transfer is now made to the beginning of the next time step to repeat the process.

B. Numerical Error Analysis of Piston Motion Simulation

The analysis of the data from the ballistic piston compressor consists of using the experimental data as target optimization by the BCCC.

The BCCC takes as input initial guesses of the thermodynamic parameters, and the experimental results of pressure, volume, and temperature as functions of time. Computational use of the experimental data is made after each simulation of the motion of the piston and physical state of the gases in the ballistic piston compressor. The experimental data is used to assign error criteria to the numerical simulation. Since different parameters will be compared for error, fractional errors will be used.

The origins in time of the numerical and experimental data are different. The origin of the experimental data coincides with the piston entering the high pressure test section. The origin of the numerical simulation coincides with the initiation of the firing sequence. The experimental and numerical data must be aligned in time before they can be compared. The offset between the two origins is approximated by considering the experimental and numerical minimum volumes and maximum pressures. The first offset is the difference in time between the experimental and numerical maximum pressures. The second offset is the difference in time between the experimental and numerical minimum volumes. The final alignment is determined by taking the average of these two offsets. Fractional errors are then assigned to those calculated data points which correspond to experimental data points. If no calculated data point falls exactly on an experimental point, one is obtained by linear interpolation between the two adjacent calculated points.

The expression for the first alignment by maximum pressures is:

$$\Delta t_p = t_{pc} - t_{pe} \quad (42)$$

where Δt_p is the alignment offset between the experimental and the calculated times of maximum pressure. t_{pe} and t_{pc} are respectively the experimental and calculated times of maximum pressure.

The expression for the second alignment by minimum volume is:

$$\Delta t_v = t_{vc} - t_{ve} \quad (43)$$

where the subscript v now implies minimum volume.

The average alignment offset is then:

$$\Delta t = (\Delta t_p + \Delta t_v)/2 \quad (44)$$

As explained previously, there is a time lag between the minimum volume and maximum pressure, the latter occurring first.

The first error point is assigned to the difference in the calculated and experimental time lags.

$$e_1 = w((t_{vc} - t_{pc}) - (t_{ve} - t_{pe})) / (t_{ve} - t_{pe}) \quad (45)$$

w is the weight assigned to this error point.

The second error point is the fractional error of the calculated and experimental maximum pressures:

$$e_2 = 2(P_e - P_c)/P_e \quad (46)$$

where P_e and P_c are the experimental and calculated maximum pressures, respectively. The third error point is the calculated and experimental minimum volumes:

$$e_3 = 2(V_e - V_c)/V_e \quad (47)$$

where V_e and V_c are the experimental and calculated minimum volumes respectively. The weighting factor for these errors is two.

Next fractional errors are assigned to the pressure and volume data points:

$$e_{3+n} = (P_e(t_n) - P_c(t_n))/P_e(t_n) \quad j \quad n=1,2,\dots,N \quad (48)$$

$$e_{3+N+j} = (V_e(t_j) - V_c(t_j))/V_e(t_j) \quad j \quad j=1,2,\dots,J \quad (49)$$

where there are N pressure points and as many volume points.

Fractional errors are then assigned to the temperature points:

$$e_{3+2N+m} = (T_e(t_m) - T_c(t_m))/T_e(t_m) \quad m=1,2,\dots,M \quad (50)$$

The weighting factor for the errors assigned to the data points after the first three is one.

A total error is also supplied the optimization program;

$$\epsilon = \sum_{i=1}^{3+2N+M} e_i^2 \quad (51)$$

The optimization part of the BCCC, after several simulation runs, computes the numerical partial derivatives of the fractional error points to be optimized, with respect to the thermodynamic parameters.

A zero derivative with respect to any parameter would imply that that parameter has no effect upon the simulation. In that case, no optimization could be performed on that parameter. While none of the derivatives will be zero, certain parameters will characteristically effect greater change in the simulation than others. In order of

decreasing sensitivity the parameters are 1) specific heat at constant volume, 2) viscosity, and 3) Van der Waals' constants. It is to be expected then, that the Van der Waals' constants will be the hardest to optimize, while the specific heat at constant volume is the easiest.

V. DATA REDUCTION AND EXPERIMENTAL RESULTS

Optimization theory pertinent to the BCCC is presented. The Gauss method of optimization with Lagrangian constraint [9,10] is used in the BCCC. To further introduce the mechanics of the BCCC, a very brief description of the input data required by the BCCC is presented.

The BCCC is capable of compensating for conditions not explicitly incorporated, such as the irregular shape of the piston, non-streamline flow, or boundary layer effects. This compensation is achieved by calibration of the BCCC.

A. Method of Optimization

The process by which the thermodynamic parameters are determined is one of optimization. Initial values of these parameters are required and obtained by an initial estimate. The fractional errors of the calculated data points with respect to the experimental results are used to modify these parameters by an appropriate logic scheme.

To be more useful, such a logic scheme for parameter optimization must have a limit on the hypersphere being searched, or in other words, a boundary must be set on the values the parameters may take. In the BCCC, these limits are in the form of a one dimensional radius about the initial value of each parameter P_i .

$$P_i \pm \Delta P_i \quad (51)$$

where P_i is the initial value of parameter P_i . It follows then that the degree of the hypersphere being searched is equal to the number

of parameters being optimized.

As explained in the previous chapter, the sum of the square of the errors is minimized,

$$\epsilon = \sum_{i=1}^{3+2N+M} e_i^2 \quad (52)$$

Taking the partial derivative of these errors with respect to each parameter being optimized gives

$$0 = \nabla \epsilon = 2 \nabla_e (P_i) e^T (P_i + \Delta P_i) \quad (53)$$

where it is assumed that the derivative $\nabla \epsilon$ remains essentially constant over the proposed step size. Expanding the right side gives

$$0 = 2 \nabla_e (P_i) [e^T (P_i) + \nabla e^T (P_i) \Delta P_i] \quad (54)$$

In order to prevent the coefficient of ΔP_i , the step size, from getting too small forcing a larger ΔP_i (as yet of unspecified width) a constant is now added to impose a minimum size on the coefficient of ΔP_i .

$$0 = \nabla e (P_i) \times e^T (P_i) + \nabla e \nabla_e^T (P_i) \Delta P_i - \lambda \bar{I} \Delta P_i \quad (55)$$

where \bar{I} is the unit matrix, and λ is the minimum coefficient of ΔP_i . Solving for ΔP_i gives:

$$\Delta P_i = -\nabla e (P_i) e^T (P_i) [\nabla e (P_i) \nabla_e^T (P_i) - \lambda \bar{I}]^{-1} \quad (56)$$

The method described above is the Gauss Method with Lagrangian Constraint. A standardized program exists at the University of Florida to implement this technique and is incorporated into the BCCC.

B. Organization of the Ballistic Compressor Computer Code

Organization of the ballistic compressor computer code, in terms of input, consists of four tables. The first table provides constraints to the parameter optimization section, such as the maximum number of steps to be taken in the hypersphere. The second table contains all parameters which may be optimized. The third table specifies the dimensions of the search hypersphere. The fourth table contains constants which are not optimized, and the experimental data points.

From this initial information, the search program calculates, by methods previously described, to the set of coordinates in the parameter hypersphere having the smallest error. The accuracy of this final coordinate is a function of the number of steps allowed the search program, the accuracy of the initial parameters, and the reliability of the experimental data.

The accuracy of the numerical model must also be included in the error analysis. Table 4 gives the results of a numerical simulation with no gas leakage or heat loss. Also listed are the initial conditions of the simulation. The close correspondence in the ideal case satisfies the requirement that the BCCC in the limit of the ideal case must reproduce theoretical answers.

C. Calibration of the BCCC

Calibration of the BCCC makes numerical allowance for those processes which have not been considered explicitly in the BCCC. Included are the irregular shape of the piston, non-streamline flow, and boundary layer effects between the test gas and the barrel wall.

The calibration of the BCCC is done by adjusting the numerical

Table 4

Results of Numerical Simulation
Without Gas Leakage or Heat Loss

INITIAL CONDITIONS

P(reservoir) = 15.3 atm

P(Helium as test gas) = 1.00 atm

P(UF₆ as test gas) = 0.00 atm

T(Temperature of test gas) = 300°K

v(Molar volume of test gas) = 24.62 (ℓ/mole)

Conditions at Maximum Compression

<u>Numerically Simulated</u>	<u>% Error of Ideal</u>
P(max)...417 atm	1.5
T(max)...3319 °K	1.5
v(min)... .653 ℓ/mole	1.5

value of the piston gap, the piston length, and the thermal coupling of the test gas to the barrel wall. Adjustment of the piston gap and length compensate for the turbulence and non-streamline flow of the leaking gas. Thus while the actual measured piston gap or length may serve as an initial guess, those values giving the most accurate results will in general be different. Calibration of the thermal coupling of the test gas to the barrel wall compensates for turbulence of the test gas and/or boundary layer effects. These phenomena affect the amount of heat energy which is conducted to the wall.

The calibration constants are roughly independent of the type of test gas used. Thus, once determined for specific physical conditions, they should not change for different test gases. The invariance of the calibration under change of test gas permits the separation of the thermodynamic and physical calibration parameters. By performing the calibration with a test gas of known thermodynamic parameters, the calibration constants are the only quantities under search and may be determined by themselves. Once determined, the process is reversed, and the thermodynamic parameters are searched.

D. Analysis of the Ratio of Specific Heat

Two primary mechanisms govern change in the ratio of specific heats during an experiment. The mechanism of greatest effect in experiments is the mixing of the test and reservoir gases. Figure 14 shows the number of moles of gas in the test gas chamber during a typical experiment.

The positive slope of the curve in this figure defines that period when reservoir gas leaks into the test gas chamber; negative slope

HE & UF₆ MIXTURE

INITIAL He PARTIAL PRESSURE : 0.96 atm

INITIAL UF₆ PARTIAL PRESSURE : 0.04 atm

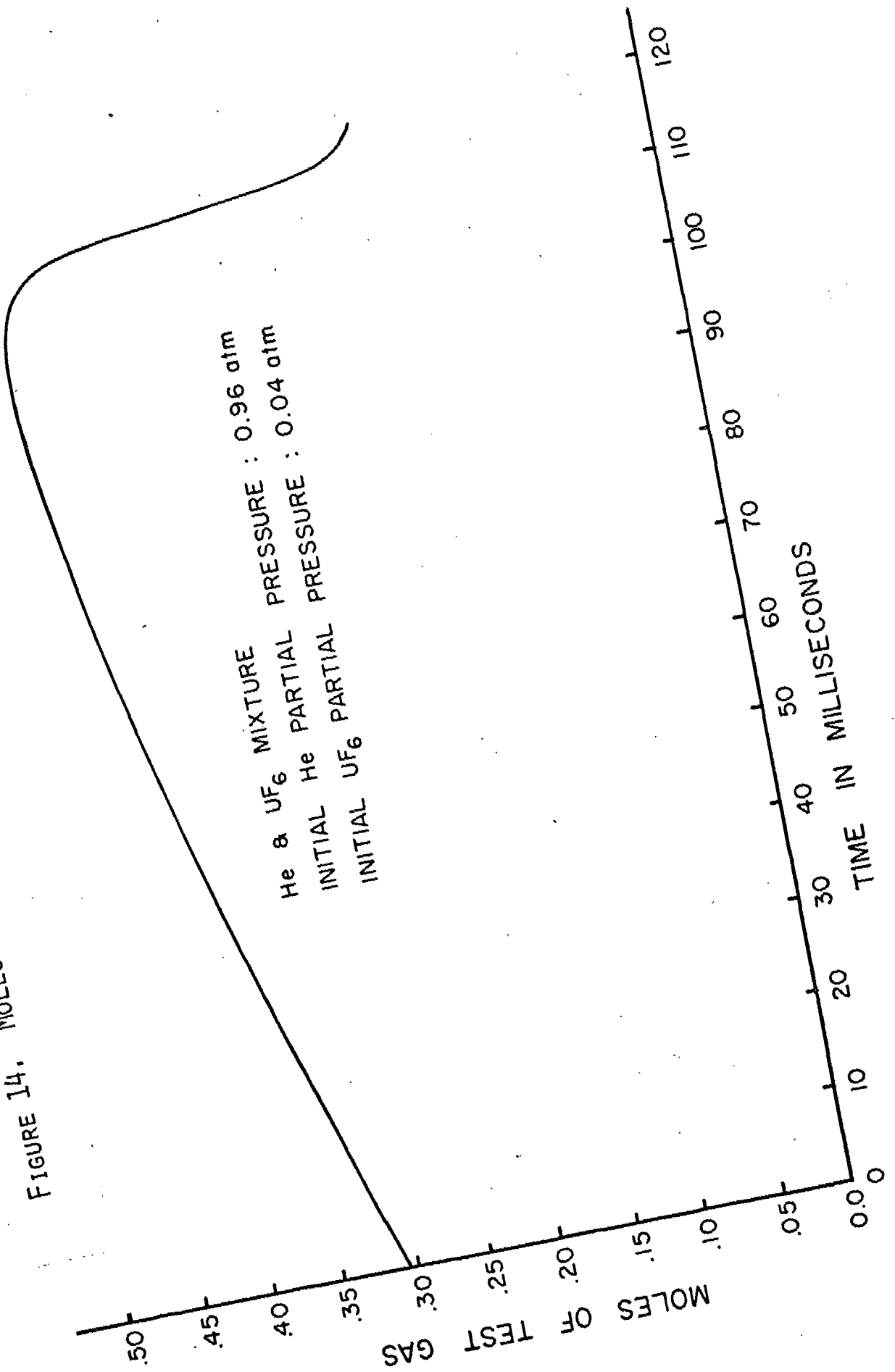


FIGURE 14. MOLES OF TEST GAS DURING A TYPICAL EXPERIMENT

implies leakage of the test gas into the reservoir. Note that while reservoir gas is leaking into the test gas chamber for well over 80% of the time, the net leakage by the end of the compression stroke is out of the test gas chamber. This results from the very high test gas pressure relative to the reservoir pressure during the latter part of the compression stroke.

Figure 15 shows an initial increase in the ratio of specific heats brought about by leakage of the helium driving gas into the test gas. This increase is terminated at the point of time when the direction of leakage reverses (i.e., when test gas pressure becomes equal to the drive pressure).

When plotted against temperature as in Figure 16, the ratio shows the same sharp increase for the same reasons as in the case versus pressure.

Figure 17 gives the ratio of specific heats as a function of time. After the initial increase due to the leaking helium, the ratio goes through a minimum at the point of highest temperature. This decrease in the magnitude of the ratio of specific heats is a result of the increased degrees of freedom excited by the high temperatures, reflected in a higher value of the specific heat at constant volume.

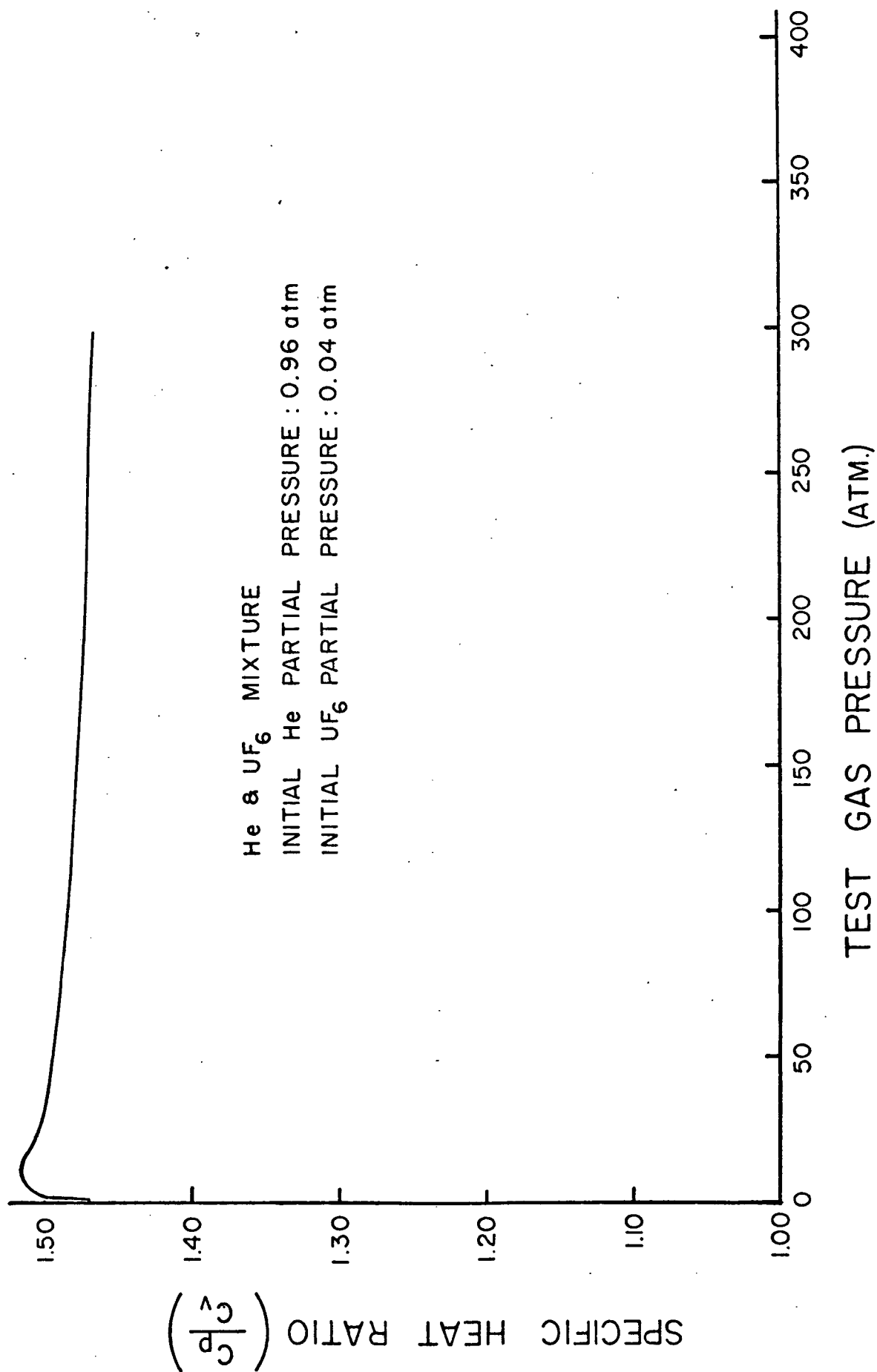
Since the ratio of specific heats of helium is still constant at the conditions under investigation, the exhibited minimum is due to the uranium hexafluoride. Table 5 lists the experimental values of specific heat (C_v) and the viscous coupling constant (C_1).

E. Analysis of the Viscous Coupling of Uranium Hexafluoride and Helium

The viscosity of uranium hexafluoride is known from 0°C to 263°C [3].

FIGURE 15.

RATIO OF SPECIFIC HEAT VS TEST GAS PRESSURE



TEST GAS PRESSURE (ATM.)

FIGURE 16. SPECIFIC HEAT RATIO VS. TEMPERATURE

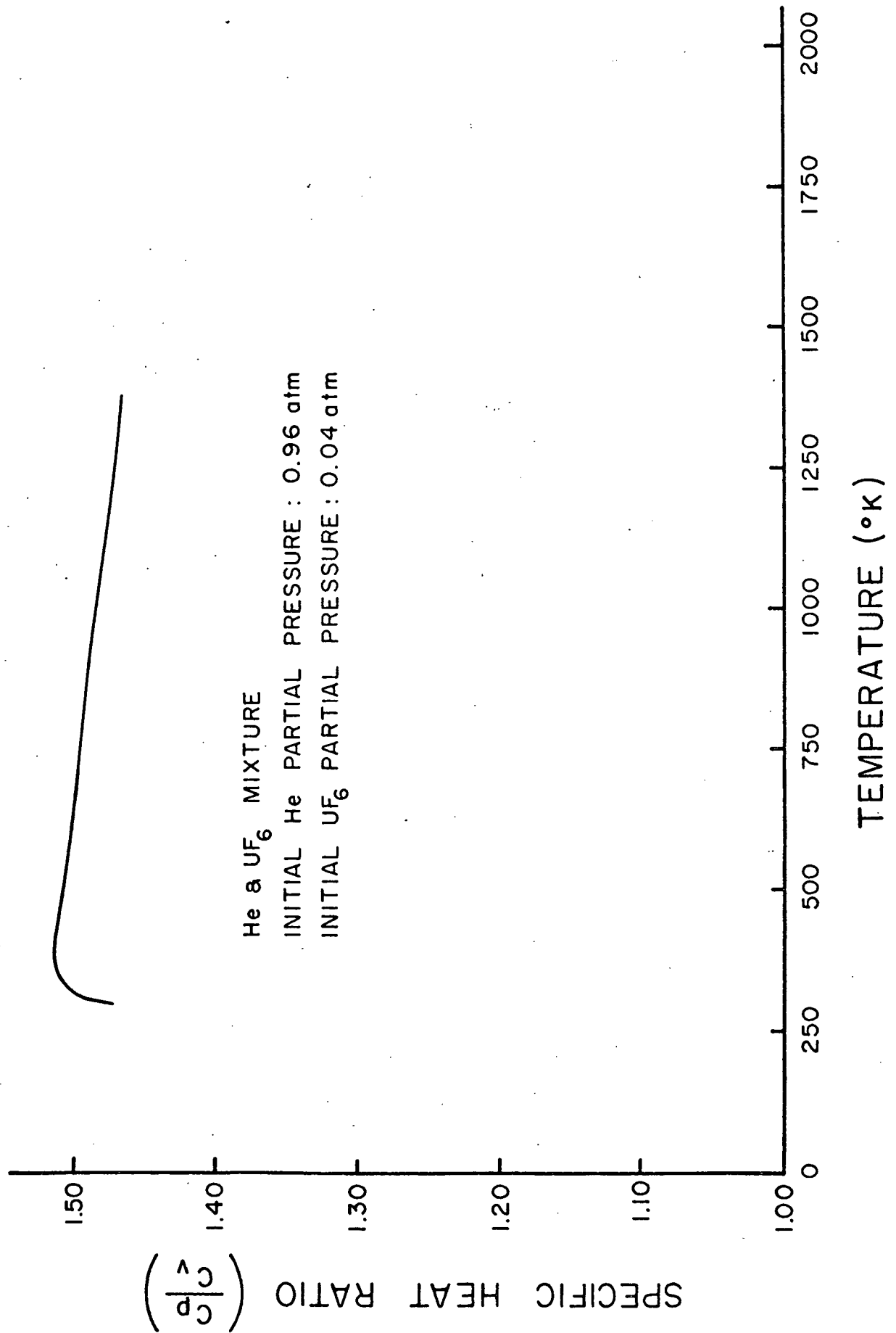


FIGURE 17. SPECIFIC HEAT RATIO VS. TIME

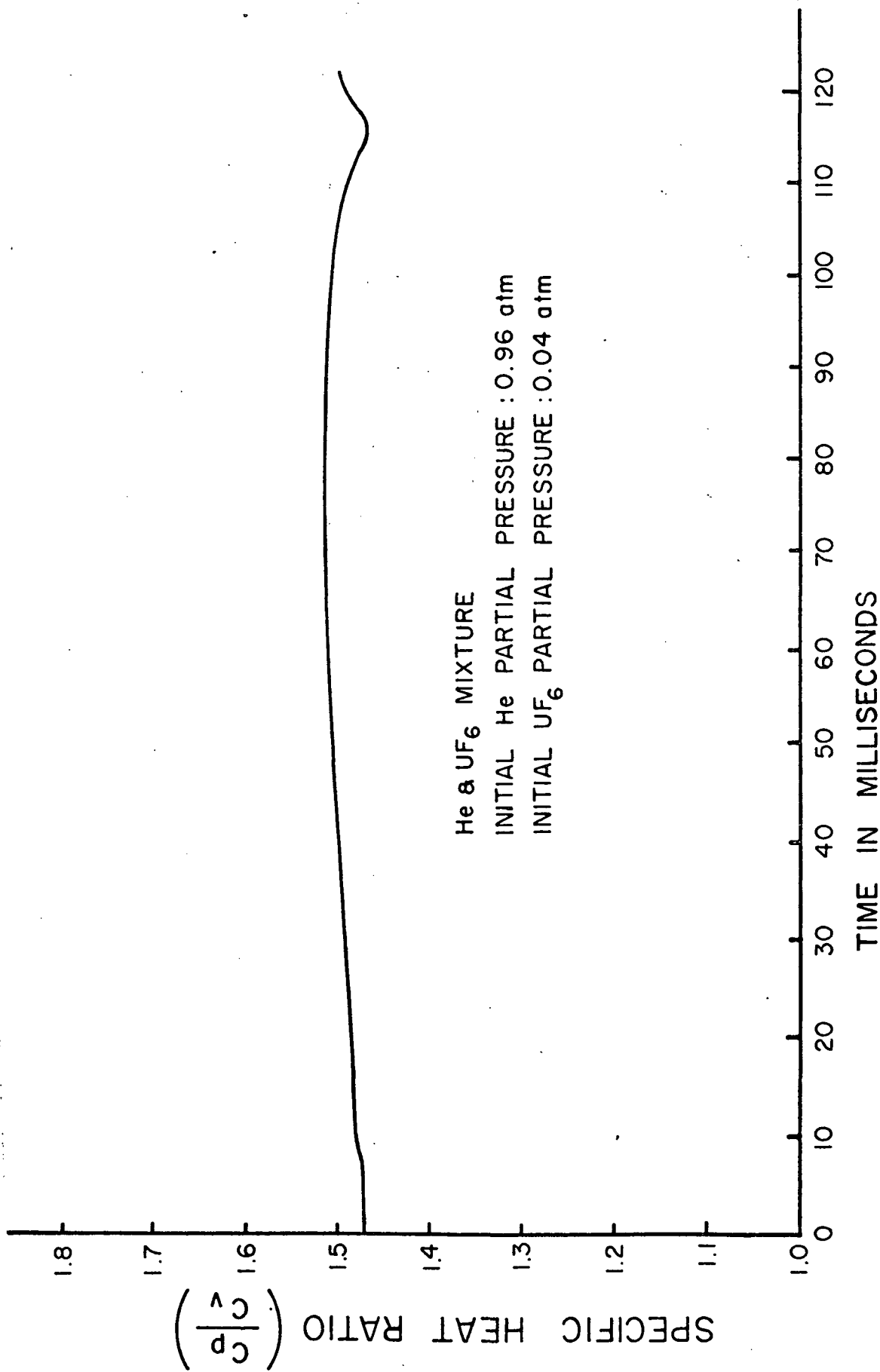


Table 5

Experimental Values of Specific Heat (C_V) and
Viscous Coupling Constant (C_1)

$$C_V(\text{UF}_6) = C_{V1} + C_{V2}T + C_{V3}T^2$$

$$(C_{V1}/R) = 13.89 \text{ R}$$

$$(C_{V2}/R^\circ\text{K}) = R/^\circ\text{K}$$

$$(C_{V3}/R^\circ\text{K}^2) = -2.10^{-6} \text{ R}/^\circ\text{K}^2$$

Viscous coupling constant of He-UF₆ mixtures:

$$C_1 = 70 \text{ } \mu\text{poise} \quad 25 \text{ } \mu\text{poise} \quad (\text{see equation 26})$$

The measurements of these investigations, fitted to the empirical formulae previously described, are extrapolated to the temperatures needed in this investigation. The viscous coupling constant C_1 is extracted by the BCCC from experimental data. The results thus far set C_1 at 70 micropoise with an estimated uncertainty of 25 micropoise (see Table 5).

Figure 18 shows the viscosity of the helium uranium hexafluoride mixture as a function of time and in Figure 19 as a function of pressure.

F. Results of Numerical Analysis of Experimental Data

The departure from a non-polytropic process has been shown to be due to heat loss to the barrel walls from the test gas, and friction work done by the leaking gas. Figure 20 is the P-V diagram of the compression process. Straight lines with slope of 1.48 are included for comparison. The average value of the slope of the experimental curve is very close to 1.48, which is also the average value of the ratio of specific heats as shown in Figure 15. One may conclude from this, that the polytropic exponent of this compression process can be approximated very closely by the ratio of specific heats (C_p/C_v).

The ratio of specific heats for pure UF_6 shown in Figure 21 as a function of temperature with pressure as parameter. The figure is computed from the measured values of the specific heat at constant volume and the Van der Waals' coefficients based on the values of the triple point of UF_6 . The dashed part of the lines in Figure 20 are not physically realized, since UF_6 is not a vapor at these conditions.

The low temperature values ($T < 500^\circ K$) of the solid lines exceed the values given in Table 1 [3], by 6%, while for temperatures greater than $500^\circ K$ our values are approximately 10% higher.

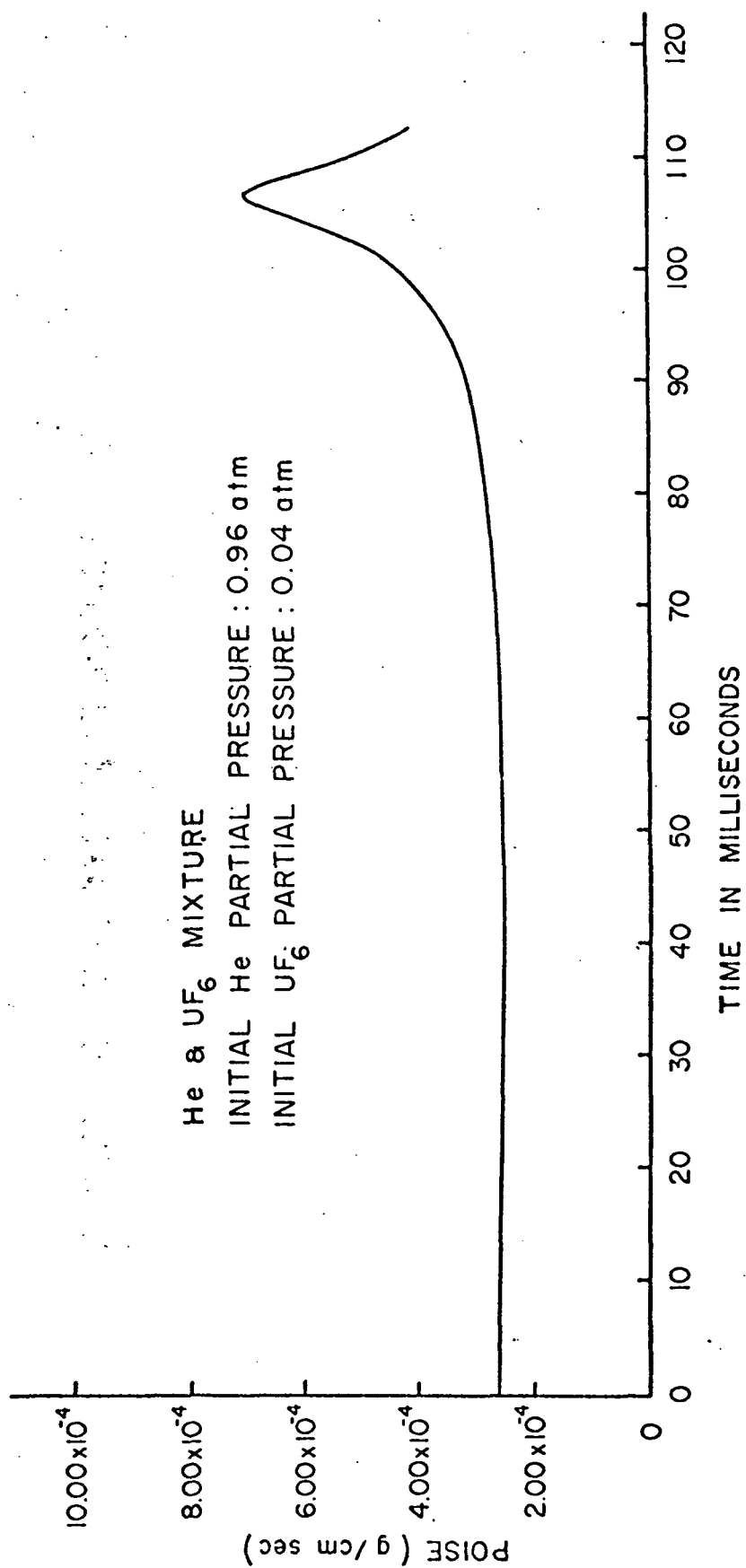


FIGURE 18. VISCOSITY OF THE TEST GAS MIXTURE

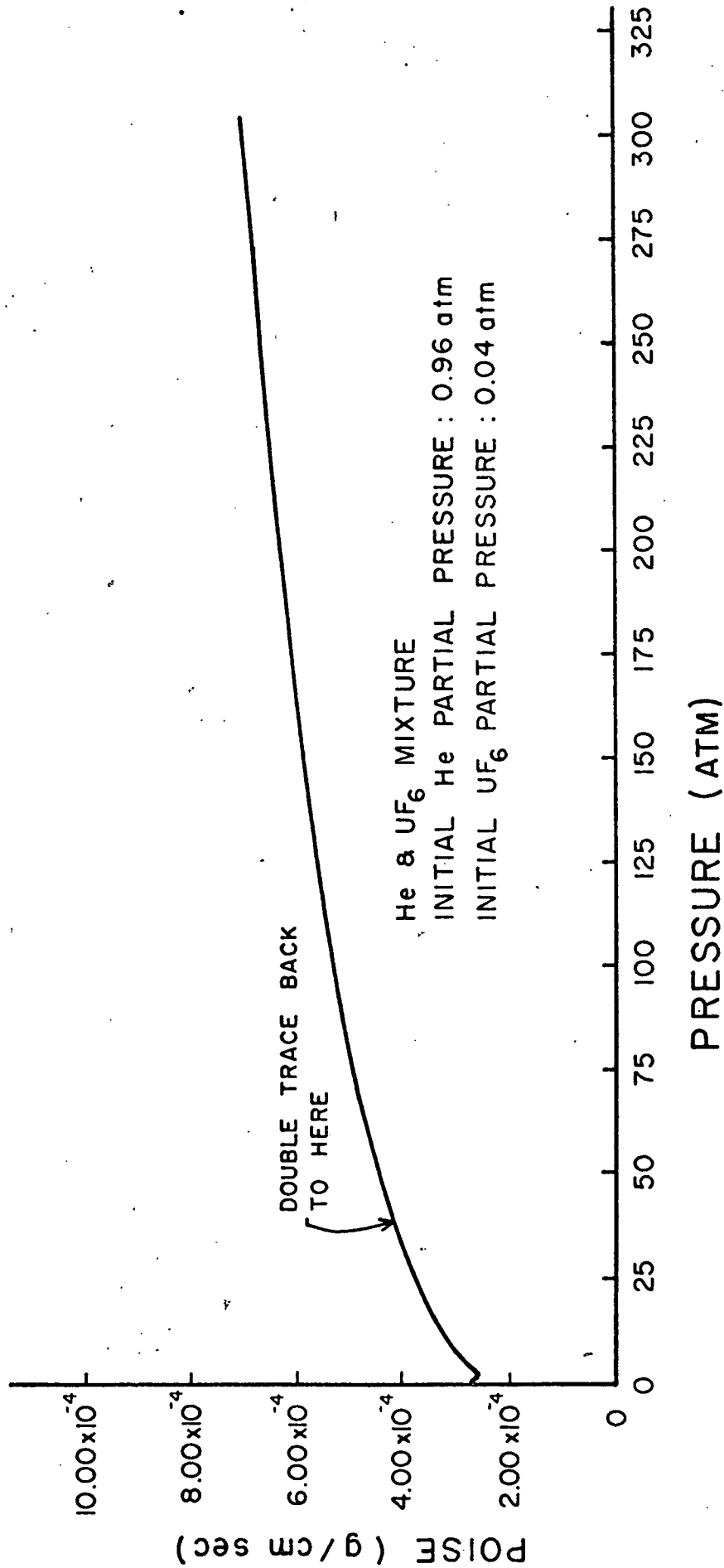
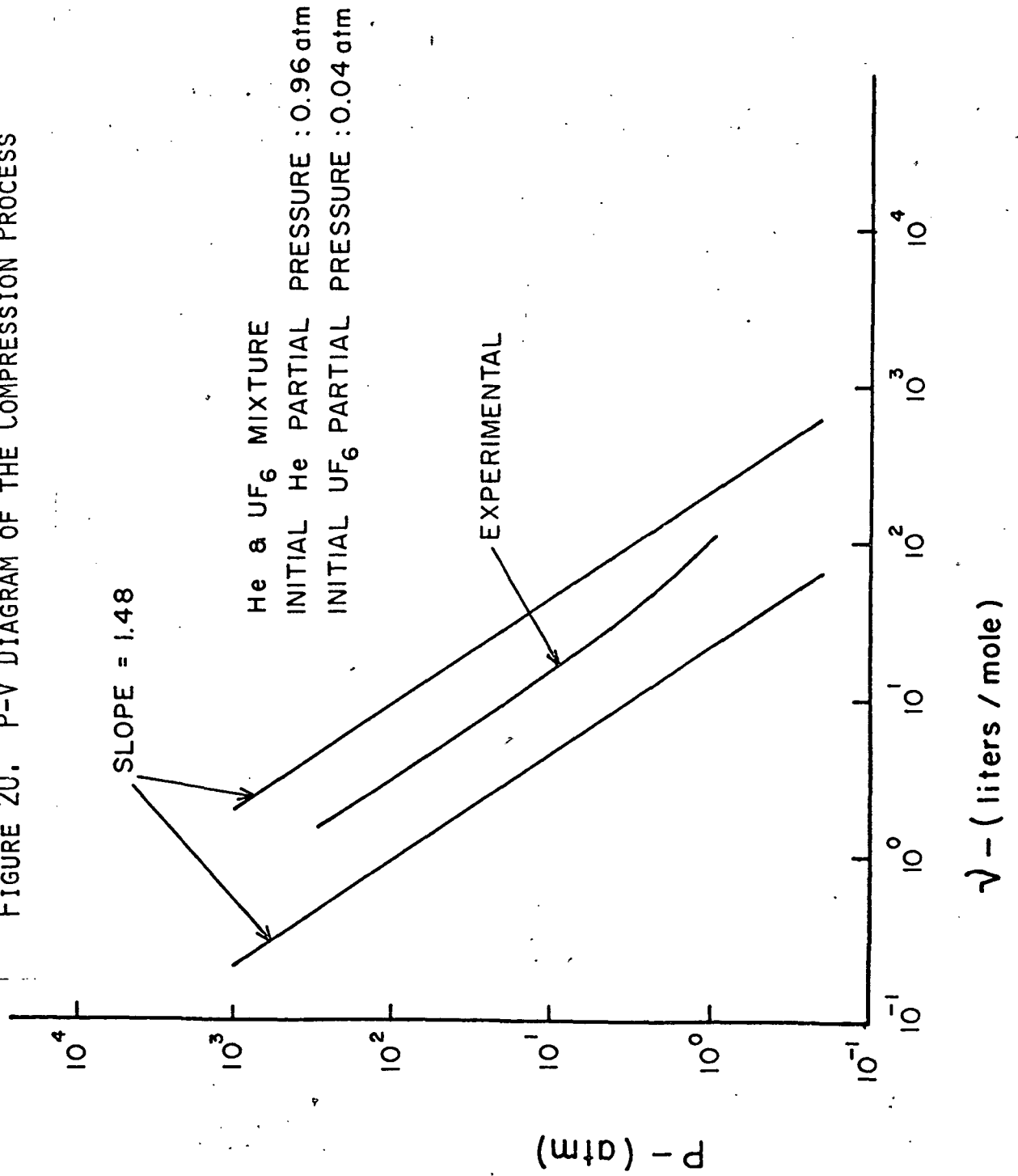


FIGURE 19. VISCOSITY OF THE TEST GAS MIXTURE AS A FUNCTION OF PRESSURE

FIGURE 20. P-V DIAGRAM OF THE COMPRESSION PROCESS



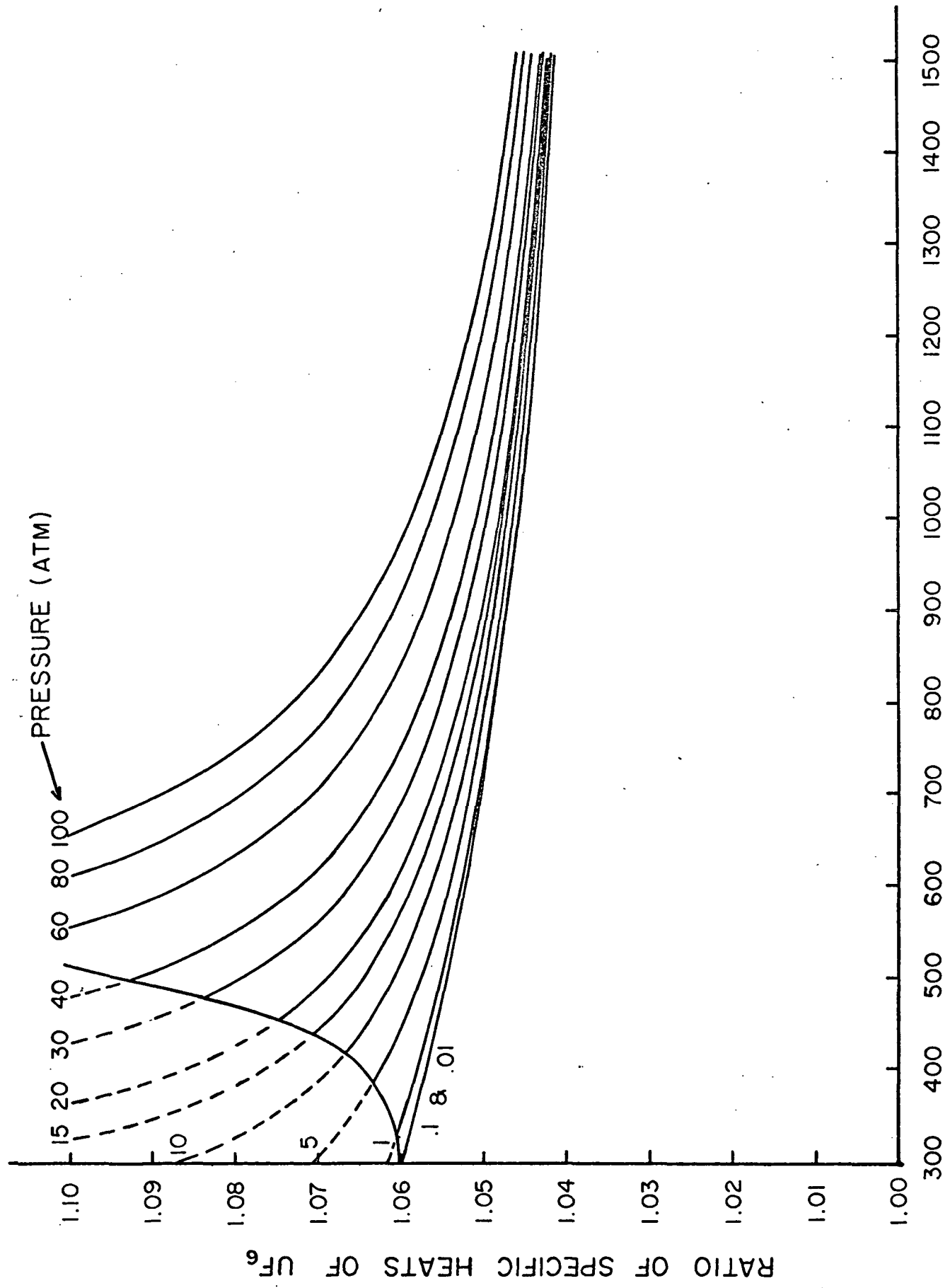


FIGURE 21. RATIO OF SPECIFIC HEATS OF URANIUM HEXAFLUORIDE

VI. CONCLUSIONS

A computer program (BCCC), capable of deriving certain thermodynamic properties of a test gas from measurements made in a ballistic piston compressor, was developed. This program was employed to determine the C_3 term (see equation 29) of the specific heat equation (C_V); the viscous coupling constant of the UF_6 (see equation 26), at experimental conditions beyond the range of previous experiments. During the course of these studies it was found that there is no significant change in the Van der Waals' constants a and b of both He and UF_6 over the range of conditions of the experiments.

The principal goal of this investigation, the measurement of specific heat ratio of pure UF_6 (see Figure 21) was accomplished by the determination of the temperature dependence of the specific heat at constant volume at high temperatures. Further analysis of the results showed, that for the He- UF_6 mixture ratios employed the polytropic exponent ($-\ln P/\ln V$) can be approximated very closely by the specific heat ratio (C_p/C_V).

Finally, it is evident that the successful implementation of the BCCC as indicated by these studies has materially enhanced the usefulness of ballistic piston compressors for investigation of physical properties of gases of high temperatures and pressures.

LIST OF REFERENCES

1. Lalos, George T. The NOL 10,000 ATM Ballistic Piston Compressor 1. Design and Construction, NOLTR 63-96. White Oak, Maryland: Naval Ordnance Laboratory, 1963.
2. Takeo, Makoto. Theoretical Analysis of the Motion of a Piston in a Ballistic Compressor. Eugene, Oregon: University of Oregon, 1965.
3. DeWitt, R. Uranium Hexafluoride: A Survey of its Physico-Chemical Properties, GAT 280. Portsmouth, Ohio: Goodyear Atomic Corporation, 1960.
4. Dmitrievskii, V.A., V.I. Fedulov, and V.F. Nikolaeva. Shock-Tube Investigation of Properties of Sulfer and Uranium Hexafluorides, Soviet Physics, JETP.
5. Lewis, M.J., B.P. Roman, G. Rovel. "Techniques for Measuring the Thermodynamic Properties of a Dense Gas," IEEE 4th International Congress on Instrumentation in Aerospace Simulation Facilities, Rhode St Genese, June 1971.
6. Lalos, George T. Private Communication.
7. Holman, J.P. Thermodynamics. New York: McGraw-Hill, 1969.
8. Kennard, Earle H. Kinetic Theory of Gases. New York: McGraw-Hill, 1938.
9. Wilde, Douglass J., Charles S. Beightler. Foundations of Optimization, Prentice-Hall, 1967.
10. Kylstra, C. D. Private Communication
11. Bigeleisen, J., Mayer, M.G., Stevenson, P.C. and Turkevich, J. "Vibrational Spectrum and Thermodynamic Properties of Uranium Hexafluoride Gas." J. Chem. Phys. 16, 442-5(1948). [Also reported in MDDC-1181 and A-1269]
12. Gaunt, J. "The Infrared Spectra and Molecular Structure of Some Group 6 Hexafluorides," Trans. Faraday Soc. 49, 1122-31 (1953). [Also reported in AERE-C/R-900]
13. Gaunt, J. "The Infrared Spectra and Molecular Structure of Some Group 6 Hexafluorides," Trans. Faraday Soc. 49, 1122-31 (1953). [Also reported in AERE-C/R-900] Data Calculated from expression for C_p .

14. Simon, F. Physical Properties of Uranium Hexafluoride. Oxford Univ., Great Britain, July 23, 1943. (100XR-2214) Restricted Circulation.
15. Nordsiek, et al. Specific Heat of UF₆. SAM Labs. (Dec. 1941) (A-87) Unclassified.
16. Booth, E.T., Callihan, D., Haggstrom, E. and Nordsieck, A. Specific Heat of UF₆. SAM Labs. (Dec. 1941) (A-87) Unclassified.
17. Duncan, A.B.F. The Raman Spectrum of UF₆. Columbia Univ. Apr. 5, 1943. (A-580) Declassified [Also reported in A-584].

APPENDIX A

DETAILS ON THE COMPRESSION PROCESS

Further details concerning the processes during compression can be obtained from Figures A-1, A-2 and A-3.

Figure A-1 show the rate of heat loss due to heat conduction to the barrel and end wall as a function of time. Figure A-2 shows the rate of heat loss as a function of pressure. Figure A-3 shows the rate of friction work done by the leaking gas on the piston as a function of time, according to equation 15. Positive friction work implies work done by the driving gas on the piston (during the time period while driving gas is leaking into the test gas). Negative friction work implies work done by the test gas on the piston (while leaking out of the high pressure section).

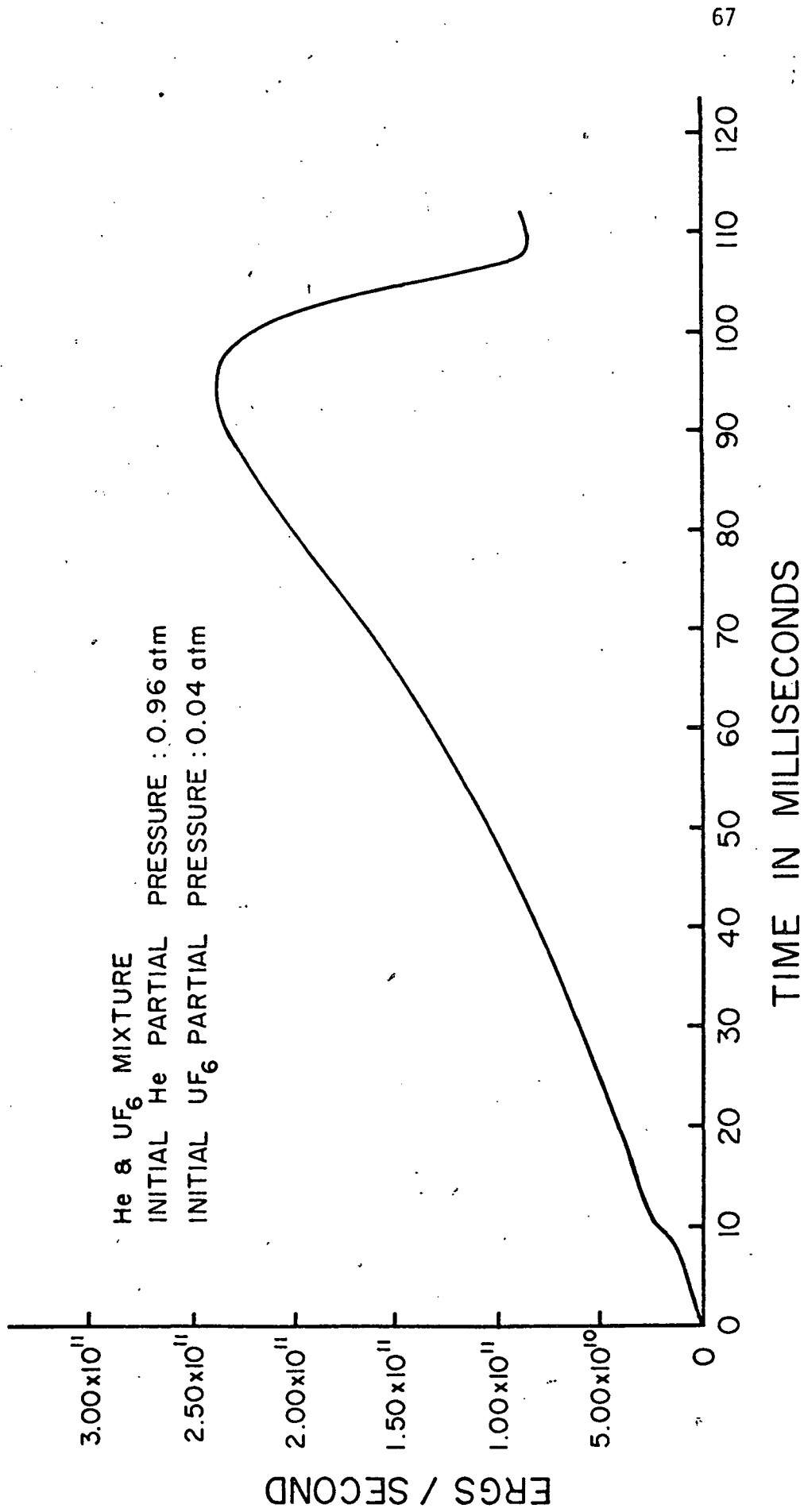


FIGURE A-1. HEAT LOSSES DURING COMPRESSION

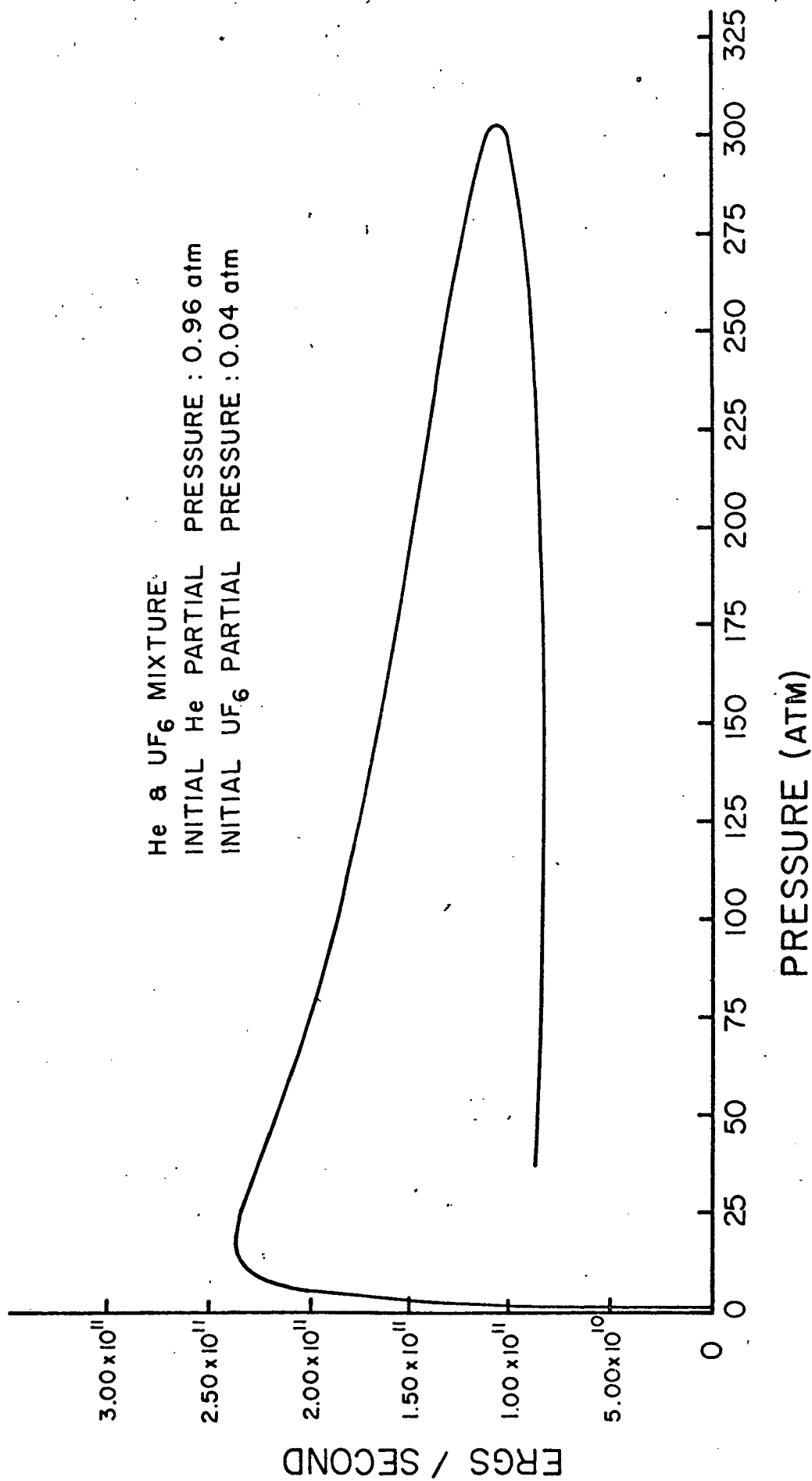


FIGURE A-2. HEAT LOSSES AS A FUNCTION OF PRESSURE

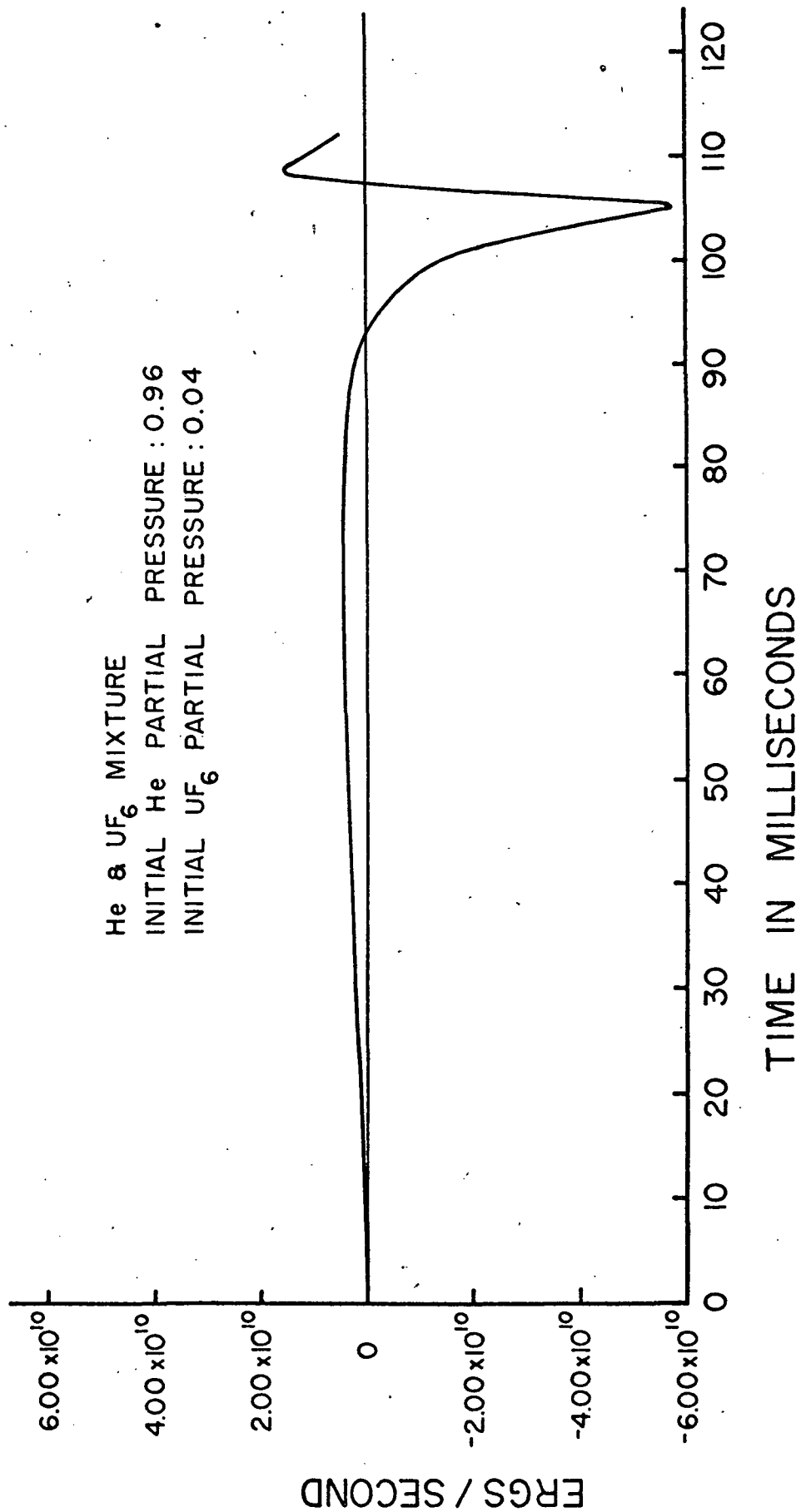


FIGURE A-3. FRICTION WORK DURING COMPRESSION

FOR A COPY OF COMPUTER PROGRAM WRITE TO:

DR. RICHARD T. SCHNEIDER
DEPARTMENT OF NUCLEAR ENGINEERING SCIENCES
202 NUCLEAR SCIENCES CENTER
UNIVERSITY OF FLORIDA
GAINESVILLE, FLORIDA, 32601